Supplementary Table 1. (Continued)

dbSNP ID	Gene symbol	Alleles	SNP bin	SNP location
rs817565	*MAPKK6*	T/G	Bin3	Intron1_21244
rs2251862	*MAPKK6*	C/A	Bin4	Exon3_8
rs2072073	*MAPKK6*	C/G	Bin5	3′flank_500
rs2716213	*MAPKK6*	T/G	Bin6	Intron1_86422
rs12451722	*MAPKK6*	T/C	Bin7	Intron1_23084
rs6501326	*MAPKK6*	A/G	Bin8	Intron1_31727
rs2716225	*MAPKK6*	G/A	Bin9	Intron1_56816
rs8080760	*MAPKK6*	A/G	Bin10	Intron1_45400
rs12948059	*MAPKK6*	A/G	Bin11	Intron1_83353
rs2074027	*MAPKK6*	A/G	Bin12	Intron2_151
rs2716222	*MAPKK6*	C/T	Bin13	Intron1_75110
rs4968857	*MAPKK6*	T/C	Bin14	Intron1_9292
rs756944	*MAPKK6*	T/C	Bin15	Intron10_8385
rs2715806	*MAPKK6*	G/A	Bin16	Intron1_48526
rs8078890	*MAPKK6*	A/C	Bin17	Intron1_71173
rs2716191	*MAPKK6*	C/T	Bin18	Intron11_4021
rs2715812	*MAPKK6*	C/T	Bin19	Intron1_57430
rs11869073	*MAPKK6*	A/C	Bin20	Intron1_65672
rs12945375	*MAPKK6*	A/G	Bin21	Intron1_58307
rs12939509	*MAPKK6*	A/G	Bin22	Intron1_38245
rs8082399	*MAPKK6*	G/A	Bin23	Intron1_3166
rs2716195	*MAPKK6*	G/A	Bin24	Intron10_5581
rs2716223	*MAPKK6*	G/A	Bin25	Intron1_75080
rs2715810	*MAPKK6*	G/A	Bin26	Intron1_40643
rs7213686	*MAPKK6*	T/C	Bin27	Intron1_42333
rs8067307	*MAPKK6*	C/A	Bin28	Intron10_5994
rs4968859	*MAPKK6*	A/C	Bin29	Intron1_47927
rs9893349	*MAPKK6*	G/A	Bin30	Intron1_62870
rs17690015	*MAPKK6*	G/A	Bin31	Intron1_51658
rs2715834	*MAPKK6*	G/C	Bin32	Intron10_5872
rs1548444	*MAPKK6*	T/G	Bin33	Intron1_65966
rs2715817	*MAPKK6*	T/C	Bin34	Intron1_71609
rs2715832	*MAPKK6*	T/C	Bin35	Intron10_4665
rs7761118	p38 MAP kinase	G/A	Bin1	Intron9_4460
rs2145362	p38 MAP kinase	C/G	Bin2	Intron3_2031
rs3752525	p38 MAP kinase	G/T	Bin3	Intron10_245
rs3730326	p38 MAP kinase	G/T	Bin4	Intron5_210
rs7770710	p38 MAP kinase	C/T	Bin5	Intron2_2152
rs16884694	p38 MAP kinase	G/A	Bin6	Intron8_18777
rs13196204	p38 MAP kinase	T/G	Bin7	Intron1_2726
rs3804453	p38 MAP kinase	A/G	Bin8	Exon12_542
rs3804454	p38 MAP kinase	T/G	Bin9	Intron1_10948
rs10807156	p38 MAP kinase	A/T	Bin10	Intron1_8809
rs4844550	*MAPKAPK2*	A/G	Bin1	5′flank_-882
rs10863784	*MAPKAPK2*	C/G	Bin2	Intron1_12931
rs12028997	*MAPKAPK2*	C/T	Bin3	Intron1_23505
rs4073250	*MAPKAPK2*	C/T	Bin4	Exon8_59
rs4072677	*MAPKAPK2*	T/G	Bin5	Intron1_20269
rs12060808	*MAPKAPK2*	C/T	Bin7	Intron1_18484
rs616589	*MAPKAPK3*	G/A	Bin1	Intron2_8414
rs3792323	*MAPKAPK3*	A/T	Bin2	Intron2_5116
rs3804628	*MAPKAPK3*	G/A	Bin3	Intron2_6866
rs2040397	*MAPKAPK3*	C/T	Bin4	Intron2_14863

Supplementary Table 2. Genotyping Results of 116 Tagging-SNPs

				All patients with HCV infection			Patients with HCV genotype 1b		
		Alleles		No. of genotypes (%)			No. of genotypes (%)		
SNP	Gene	(1/2)	Group	1/1	1/2	2/2	1/1	1/2	2/2
rs2243594	*IFNAR1*	A/G	SR	210 (45.1)	213 (45.7)	43 (9.2)	94 (50.3)	93 (49.7)	20 (10.7)
			NR	263 (45.2)	245 (42.1)	74 (12.7)	198 (50.3)	176 (44.7)	55 (14)
rs2243600	*IFNAR1*	G/T	SR	128 (27.5)	223 (47.9)	115 (24.7)	62 (30)	101 (48.8)	44 (21.3)
			NR	163 (28)	300 (51.5)	120 (20.6)	119 (27.7)	217 (50.5)	94 (21.9)
rs2252930	*IFNAR1*	C/G	SR	298 (63.8)	152 (32.5)	17 (3.6)	125 (60.1)	75 (36.1)	8 (3.8)
			NR	362 (62.2)	191 (32.8)	29 (5)	274 (63.9)	134 (31.2)	21 (4.9)
rs2252650	*IFNAR2*	A/T	SR	145 (31)	227 (48.6)	95 (20.3)	63 (30.4)	101 (48.8)	43 (20.8)
			NR	168 (28.7)	293 (50)	125 (21.3)	119 (27.5)	219 (50.6)	95 (21.9)
rs6517154	*IFNAR2*	T/C	SR	413 (88.6)	50 (10.7)	3 (0.6)	181 (87.4)	24 (11.6)	2 (1)
			NR	509 (86.9)	76 (13)	1 (0.2)	378 (87.3)	54 (12.5)	1 (0.2)
rs2073362	*IFNAR2*	A/G	SR	338 (73)	116 (25.1)	9 (1.9)	149 (72.7)	52 (25.4)	4 (2)
			NR	452 (77.4)	121 (20.7)	11 (1.9)	341 (79.1)	84 (19.5)	6 (1.4)
rs2248202	*IFNAR2*	A/C	SR	183 (39.4)	210 (45.3)	71 (15.3)	80 (39)	96 (46.8)	29 (14.1)
			NR	218 (37.2)	274 (46.8)	94 (16)	155 (35.8)	205 (47.3)	73 (16.9)
rs10211925	*IFNAR2*	G/A	SR	436 (94.4)	26 (5.6)	0 (0)	189 (91.7)	17 (8.3)	0 (0)
			NR	553 (95.2)	27 (4.6)	1 (0.2)	412 (95.6)	18 (4.2)	1 (0.2)
rs2248412	*IFNAR2*	A/G	SR	269 (57.5)	166 (35.5)	33 (7.1)	114 (54.8)	81 (38.9)	13 (6.3)
			NR	313 (53.4)	232 (39.6)	41 (7)	228 (52.5)	177 (40.8)	29 (6.7)
rs310209	*JAK1*	C/A	SR	240 (51.6)	182 (39.1)	43 (9.2)	109 (52.7)	76 (36.7)	22 (10.6)
			NR	293 (49.9)	251 (42.8)	43 (7.3)	208 (47.9)	190 (43.8)	36 (8.3)
rs3790541	*JAK1*	C/T	SR	239 (51.2)	189 (40.5)	39 (8.4)	99 (47.6)	85 (40.9)	24 (11.5)
			NR	295 (50.5)	245 (42)	44 (7.5)	220 (50.8)	177 (40.9)	36 (8.3)
rs310247	*JAK1*	A/G	SR	147 (31.5)	233 (49.9)	87 (18.6)	72 (34.6)	105 (50.5)	31 (14.9)
			NR	180 (30.8)	295 (50.5)	109 (18.7)	140 (32.4)	220 (50.9)	72 (16.7)
rs3790532	*JAK1*	G/A	SR	252 (54.3)	175 (37.7)	37 (8)	114 (55.3)	74 (35.9)	18 (8.7)
			NR	317 (54)	232 (39.5)	38 (6.5)	224 (51.6)	176 (40.6)	34 (7.8)
rs2254002	*JAK1*	A/C	SR	158 (33.8)	230 (49.1)	80 (17.1)	74 (35.6)	106 (51)	28 (13.5)
			NR	186 (31.7)	304 (51.8)	97 (16.5)	145 (33.4)	225 (51.8)	64 (14.7)
rs3818753	*JAK1*	A/G	SR	405 (86.5)	59 (12.6)	4 (0.9)	173 (83.2)	31 (14.9)	4 (1.9)
			NR	532 (90.9)	53 (9.1)	0 (0)	389 (89.8)	44 (10.2)	0 (0)
rs17127024	*JAK1*	G/T	SR	310 (66.4)	134 (28.7)	23 (4.9)	141 (67.8)	56 (26.9)	11 (5.3)
			NR	369 (62.9)	194 (33)	24 (4.1)	276 (63.6)	142 (32.7)	16 (3.7)
rs2274948	*JAK1*	T/C	SR	358 (77)	98 (21.1)	9 (1.9)	154 (74.8)	48 (23.3)	4 (1.9)
			NR	424 (72.9)	153 (26.3)	5 (0.9)	312 (72.2)	115 (26.6)	5 (1.2)
rs280523	Tyrosine kinase2	G/A	SR	416 (89.3)	47 (10.1)	3 (0.6)	182 (87.9)	25 (12.1)	0 (0)
			NR	520 (88.6)	66 (11.2)	1 (0.2)	387 (89.2)	46 (10.6)	1 (0.2)
rs280519	Tyrosine kinase2	A/G	SR	134 (28.8)	241 (51.7)	91 (19.5)	58 (27.9)	113 (54.3)	37 (17.8)
			NR	166 (28.4)	293 (50.1)	126 (21.5)	130 (30)	208 (48)	95 (21.9)
rs280496	Tyrosine kinase2	C/G	SR	391 (83.5)	75 (16)	2 (0.4)	172 (82.7)	36 (17.3)	0 (0)
			NR	485 (82.6)	96 (16.4)	6 (1)	360 (82.9)	69 (15.9)	5 (1.2)
rs11885069	*STAT1*	C/T	SR	363 (78.1)	93 (20)	9 (1.9)	155 (75.2)	46 (22.3)	5 (2.4)
			NR	466 (79.5)	115 (19.6)	5 (0.9)	335 (77.4)	94 (21.7)	4 (0.9)
rs9789428	*STAT1*	C/A	SR	415 (88.7)	51 (10.9)	2 (0.4)	182 (87.5)	24 (11.5)	2 (1)
			NR	523 (89.4)	61 (10.4)	1 (0.2)	384 (88.9)	47 (10.9)	1 (0.2)
rs2280233	*STAT1*	T/C	SR	339 (72.6)	124 (26.6)	4 (0.9)	161 (77.8)	45 (21.7)	1 (0.5)
			NR	444 (75.8)	133 (22.7)	9 (1.5)	331 (76.4)	95 (21.9)	7 (1.6)
rs13395505	*STAT1*	A/G	SR	173 (37)	216 (46.3)	78 (16.7)	88 (42.5)	86 (41.5)	33 (15.9)
			NR	227 (38.7)	269 (45.8)	91 (15.5)	172 (39.6)	195 (44.9)	67 (15.4)
rs12693589	*STAT1*	C/T	SR	130 (27.8)	229 (48.9)	109 (23.3)	69 (33.2)	91 (43.8)	48 (23.1)
			NR	164 (27.9)	301 (51.3)	122 (20.8)	124 (28.6)	221 (50.9)	89 (20.5)
rs2066805	*STAT1*	T/C	SR	436 (93.2)	32 (6.8)	0 (0)	197 (94.7)	11 (5.3)	0 (0)
			NR	533 (91)	51 (8.7)	2 (0.3)	395 (91.2)	36 (8.3)	2 (0.5)
rs1400657	*STAT1*	T/G	SR	356 (76.1)	100 (21.4)	12 (2.6)	170 (81.7)	35 (16.8)	3 (1.4)
			NR	441 (75.3)	129 (22)	16 (2.7)	338 (78.1)	85 (19.6)	10 (2.3)
rs3771300	*STAT1*	T/G	SR	246 (52.6)	185 (39.5)	37 (7.9)	110 (52.9)	78 (37.5)	20 (9.6)
			NR	327 (56.2)	216 (37.1)	39 (6.7)	236 (54.9)	163 (37.9)	31 (7.2)
rs11677408	*STAT1*	C/T	SR	393 (84.2)	70 (15)	4 (0.9)	170 (82.1)	35 (16.9)	2 (1)
			NR	500 (85.3)	82 (14)	4 (0.7)	361 (83.4)	69 (15.9)	3 (0.7)
rs11887698	*STAT1*	A/G	SR	260 (55.6)	171 (36.5)	37 (7.9)	110 (52.9)	80 (38.5)	18 (8.7)
			NR	344 (58.6)	217 (37)	26 (4.4)	245 (56.5)	167 (38.5)	22 (5.1)

Supplementary Table 2. (Continued)

SNP	Gene	Alleles (1/2)	Group	All patients with HCV infection: No. of genotypes (%) 1/1	1/2	2/2	Patients with HCV genotype 1b: No. of genotypes (%) 1/1	1/2	2/2
rs2030171	*STAT1*	A/G	SR	214 (46.1)	202 (43.5)	48 (10.3)	105 (51)	80 (38.8)	21 (10.2)
			NR	268 (45.9)	252 (43.2)	64 (11)	203 (47.1)	181 (42)	47 (10.9)
rs1467199	*STAT1*	C/G	SR	119 (25.6)	236 (50.9)	109 (23.5)	44 (21.5)	101 (49.3)	60 (29.3)
			NR	162 (27.9)	286 (49.2)	133 (22.9)	115 (26.7)	215 (50)	100 (23.3)
rs10199181	*STAT1*	T/A	SR	231 (49.4)	189 (40.4)	48 (10.3)	115 (55.3)	75 (36.1)	18 (8.7)
			NR	286 (48.9)	245 (41.9)	54 (9.2)	222 (51.3)	174 (40.2)	37 (8.5)
rs2066802	*STAT1*	A/G	SR	288 (62.5)	149 (32.3)	24 (5.2)	128 (63.7)	64 (31.8)	9 (4.5)
			NR	373 (64)	179 (30.7)	31 (5.3)	271 (63)	136 (31.6)	23 (5.3)
rs16833155	*STAT1*	C/T	SR	436 (93.4)	31 (6.6)	0 (0)	196 (94.7)	11 (5.3)	0 (0)
			NR	531 (91.1)	50 (8.6)	2 (0.3)	394 (91.4)	35 (8.1)	2 (0.5)
rs2066799	*STAT1*	C/T	SR	391 (83.5)	70 (15)	7 (1.5)	169 (81.3)	35 (16.8)	4 (1.9)
			NR	496 (84.6)	86 (14.7)	4 (0.7)	358 (82.7)	72 (16.6)	3 (0.7)
rs11693463	*STAT1*	A/G	SR	338 (72.4)	118 (25.3)	11 (2.4)	148 (71.5)	53 (25.6)	6 (2.9)
			NR	419 (71.6)	153 (26.2)	13 (2.2)	303 (70)	119 (27.5)	11 (2.5)
rs10208033	*STAT1*	C/T	SR	208 (44.5)	212 (45.4)	47 (10.1)	95 (45.9)	92 (44.4)	20 (9.7)
			NR	276 (47.2)	254 (43.4)	55 (9.4)	201 (46.5)	191 (44.2)	40 (9.3)
rs3755312	*STAT1*	C/G	SR	336 (71.8)	118 (25.2)	14 (3)	142 (68.3)	57 (27.4)	9 (4.3)
			NR	447 (76.7)	127 (21.8)	9 (1.5)	317 (73.5)	107 (24.8)	7 (1.6)
rs2280232	*STAT1*	A/C	SR	337 (72.2)	119 (25.5)	11 (2.4)	157 (75.8)	46 (22.2)	4 (1.9)
			NR	397 (68)	171 (29.3)	16 (2.7)	295 (68.4)	125 (29)	11 (2.6)
rs13029532	*STAT1*	A/C	SR	354 (76.1)	102 (21.9)	9 (1.9)	165 (79.7)	38 (18.4)	4 (1.9)
			NR	426 (72.8)	145 (24.8)	14 (2.4)	322 (74.4)	99 (22.9)	12 (2.8)
rs7562024	*STAT1*	T/C	SR	370 (79.4)	94 (20.2)	2 (0.4)	174 (84.1)	32 (15.5)	1 (0.5)
			NR	459 (78.6)	116 (19.9)	9 (1.5)	349 (81)	76 (17.6)	6 (1.4)
rs1914408	*STAT1*	C/T	SR	218 (46.6)	195 (41.7)	55 (11.8)	86 (41.3)	92 (44.2)	30 (14.4)
			NR	249 (42.6)	264 (45.1)	72 (12.3)	189 (43.8)	191 (44.2)	52 (12)
rs2066807	*STAT2*	C/G	SR	424 (90.6)	43 (9.2)	1 (0.2)	189 (90.9)	18 (8.7)	1 (0.5)
			NR	523 (89.4)	60 (10.3)	2 (0.3)	392 (90.7)	40 (9.3)	0 (0)
rs12432194	IFN regulatory factor 9	C/T	SR	263 (56.4)	172 (36.9)	31 (6.7)	119 (57.5)	77 (37.2)	11 (5.3)
			NR	347 (59.1)	203 (34.6)	37 (6.3)	254 (58.5)	153 (35.3)	27 (6.2)
rs4981494	IFN regulatory factor 9	G/A	SR	202 (43.4)	211 (45.4)	52 (11.2)	95 (45.9)	91 (44)	21 (10.1)
			NR	272 (46.7)	250 (42.9)	61 (10.5)	197 (45.8)	187 (43.5)	46 (10.7)
rs12432304	IFN regulatory factor 9	C/T	SR	130 (27.9)	225 (48.3)	111 (23.8)	61 (29.5)	99 (47.8)	47 (22.7)
			NR	158 (27.2)	282 (48.6)	140 (24.1)	120 (28)	203 (47.4)	105 (24.5)
rs2277484	IFN regulatory factor 9	G/A	SR	337 (72.6)	110 (23.7)	17 (3.7)	154 (74.4)	45 (21.7)	8 (3.9)
			NR	401 (68.4)	170 (29)	15 (2.6)	295 (68)	127 (29.3)	12 (2.8)
rs2236350	IFN regulatory factor 9	C/A	SR	206 (44)	209 (44.7)	53 (11.3)	88 (42.3)	98 (47.1)	22 (10.6)
			NR	254 (43.6)	269 (46.1)	60 (10.3)	189 (43.8)	194 (44.9)	49 (11.3)
rs2303364	Ras-related C3 botulinum toxin substrate 1	C/T	SR	162 (34.8)	229 (49.2)	74 (15.9)	67 (32.5)	102 (49.5)	37 (18)
			NR	196 (33.7)	275 (47.3)	111 (19.1)	137 (31.9)	214 (49.8)	79 (18.4)
rs836483	Ras-related C3 botulinum toxin substrate 1	G/A	SR	384 (82.6)	76 (16.3)	5 (1.1)	171 (82.6)	35 (16.9)	1 (0.5)
			NR	472 (80.7)	110 (18.8)	3 (0.5)	346 (79.9)	84 (19.4)	3 (0.7)
rs6954996	Ras-related C3 botulinum toxin substrate 1	G/A	SR	412 (88.6)	51 (11)	2 (0.4)	182 (88.3)	23 (11.2)	1 (0.5)
			NR	513 (87.8)	68 (11.6)	3 (0.5)	377 (87.3)	52 (12)	3 (0.7)
rs7456834	Ras-related C3 botulinum toxin substrate 1	G/C	SR	307 (66)	144 (31)	14 (3)	133 (64.6)	62 (30.1)	11 (5.3)
			NR	370 (63.5)	197 (33.8)	16 (2.7)	270 (62.5)	151 (35)	11 (2.5)
rs702484	Ras-related C3 botulinum toxin substrate 1	G/C	SR	320 (68.5)	135 (28.9)	12 (2.6)	142 (68.3)	60 (28.8)	6 (2.9)
			NR	393 (67.2)	178 (30.4)	14 (2.4)	285 (66)	135 (31.3)	12 (2.8)
rs2347339	Ras-related C3 botulinum toxin substrate 1	C/G	SR	305 (65.3)	137 (29.3)	25 (5.4)	132 (63.8)	60 (29)	15 (7.2)
			NR	368 (63.1)	182 (31.2)	33 (5.7)	268 (62.2)	141 (32.7)	22 (5.1)
rs768409	Ras-related C3 botulinum toxin substrate 1	A/T	SR	456 (97.9)	10 (2.1)	0 (0)	202 (97.6)	5 (2.4)	0 (0)
			NR	579 (99.1)	5 (0.9)	0 (0)	428 (99.1)	4 (0.9)	0 (0)
rs2305871	*MAPKK3*	G/C	SR	241 (51.6)	202 (43.3)	24 (5.1)	104 (50.2)	89 (43)	14 (6.8)
			NR	317 (54.3)	223 (38.2)	44 (7.5)	233 (53.9)	164 (38)	35 (8.1)
rs9901404	*MAPKK3*	G/A	SR	207 (44.4)	212 (45.5)	47 (10.1)	97 (46.9)	93 (44.9)	17 (8.2)
			NR	232 (39.7)	271 (46.4)	81 (13.9)	180 (41.8)	193 (44.8)	58 (13.5)
rs12602109	*MAPKK3*	G/A	SR	167 (36)	224 (48.3)	73 (15.7)	76 (36.7)	94 (45.4)	37 (17.9)
			NR	238 (41.2)	265 (45.9)	74 (12.8)	174 (40.8)	193 (45.3)	59 (13.8)

Supplementary Table 2. (Continued)

SNP	Gene	Alleles (1/2)	Group	All patients with HCV infection No. of genotypes (%) 1/1	1/2	2/2	Patients with HCV genotype 1b No. of genotypes (%) 1/1	1/2	2/2
rs3760201	*MAPKK3*	A/G	SR	198 (42.6)	217 (46.7)	50 (10.8)	98 (47.3)	88 (42.5)	21 (10.1)
			NR	222 (38.5)	275 (47.7)	80 (13.9)	169 (39.4)	199 (46.4)	61 (14.2)
rs8074866	*MAPKK3*	C/T	SR	248 (53.2)	195 (41.8)	23 (4.9)	110 (53.1)	84 (40.6)	13 (6.3)
			NR	343 (58.9)	207 (35.6)	32 (5.5)	257 (59.6)	148 (34.3)	26 (6)
rs2074028	*MAPKK6*	T/C	SR	170 (36.5)	233 (50)	63 (13.5)	65 (31.3)	109 (52.4)	34 (16.3)
			NR	200 (34.2)	283 (48.4)	102 (17.4)	144 (33.3)	211 (48.8)	77 (17.8)
rs2034100	*MAPKK6*	G/A	SR	409 (87.6)	56 (12)	2 (0.4)	181 (87.4)	25 (12.1)	1 (0.5)
			NR	518 (88.7)	64 (11)	2 (0.3)	381 (88.2)	49 (11.3)	2 (0.5)
rs817565	*MAPKK6*	T/G	SR	125 (26.8)	214 (45.9)	127 (27.3)	66 (31.9)	87 (42)	54 (26.1)
			NR	159 (27.1)	284 (48.4)	144 (24.5)	115 (26.5)	216 (49.8)	103 (23.7)
rs2251862	*MAPKK6*	C/A	SR	231 (49.6)	193 (41.4)	42 (9)	88 (42.7)	95 (46.1)	23 (11.2)
			NR	263 (45)	259 (44.3)	62 (10.6)	186 (43)	198 (45.7)	49 (11.3)
rs2072073	*MAPKK6*	C/G	SR	239 (51.3)	183 (39.3)	44 (9.4)	112 (54.1)	76 (36.7)	19 (9.2)
			NR	272 (46.5)	264 (45.1)	49 (8.4)	204 (47.1)	196 (45.3)	33 (7.6)
rs2716213	*MAPKK6*	T/G	SR	159 (34)	222 (47.5)	86 (18.4)	58 (28)	103 (49.8)	46 (22.2)
			NR	201 (34.4)	274 (46.8)	110 (18.8)	140 (32.4)	202 (46.8)	90 (20.8)
rs12451722	*MAPKK6*	T/C	SR	304 (65.2)	145 (31.1)	17 (3.6)	141 (67.8)	56 (26.9)	11 (5.3)
			NR	382 (65.5)	177 (30.4)	24 (4.1)	283 (65.5)	129 (29.9)	20 (4.6)
rs6501326	*MAPKK6*	A/G	SR	187 (40.3)	216 (46.6)	61 (13.1)	76 (36.9)	96 (46.6)	34 (16.5)
			NR	231 (39.5)	268 (45.8)	86 (14.7)	167 (38.6)	204 (47.1)	62 (14.3)
rs2716225	*MAPKK6*	G/A	SR	345 (73.7)	108 (23.1)	15 (3.2)	152 (73.1)	46 (22.1)	10 (4.8)
			NR	437 (74.4)	141 (24)	9 (1.5)	336 (77.4)	93 (21.4)	5 (1.2)
rs8080760	*MAPKK6*	A/G	SR	143 (30.8)	233 (50.2)	88 (19)	62 (30.1)	105 (51)	39 (18.9)
			NR	177 (30.3)	294 (50.3)	114 (19.5)	131 (30.3)	213 (49.3)	88 (20.4)
rs12948059	*MAPKK6*	A/G	SR	341 (73.3)	112 (24.1)	12 (2.6)	160 (77.3)	43 (20.8)	4 (1.9)
			NR	418 (71.7)	153 (26.2)	12 (2.1)	323 (75.1)	100 (23.3)	7 (1.6)
rs2074027	*MAPKK6*	A/G	SR	156 (33.4)	223 (47.8)	88 (18.8)	79 (38)	92 (44.2)	37 (17.8)
			NR	206 (35.2)	264 (45.1)	115 (19.7)	156 (36)	188 (43.4)	89 (20.6)
rs2716222	*MAPKK6*	C/T	SR	186 (39.9)	217 (46.6)	63 (13.5)	86 (41.5)	93 (44.9)	28 (13.5)
			NR	260 (44.4)	244 (41.7)	81 (13.8)	194 (44.8)	180 (41.6)	59 (13.6)
rs4968857	*MAPKK6*	T/C	SR	144 (30.9)	232 (49.8)	90 (19.3)	77 (37.4)	88 (42.7)	41 (19.9)
			NR	192 (32.9)	275 (47.1)	117 (20)	143 (33.2)	205 (47.6)	83 (19.3)
rs756944	*MAPKK6*	T/C	SR	151 (32.5)	229 (49.2)	85 (18.3)	76 (37.1)	87 (42.4)	42 (20.5)
			NR	188 (32.2)	298 (51)	98 (16.8)	143 (33.2)	215 (49.9)	73 (16.9)
rs2715806	*MAPKK6*	G/A	SR	197 (42.5)	209 (45)	58 (12.5)	92 (44.4)	89 (43)	26 (12.6)
			NR	272 (46.5)	243 (41.5)	70 (12)	210 (48.6)	170 (39.4)	52 (12)
rs8078890	*MAPKK6*	A/C	SR	136 (29.2)	225 (48.3)	105 (22.5)	63 (30.4)	93 (44.9)	51 (24.6)
			NR	176 (30.1)	279 (47.8)	129 (22.1)	132 (30.6)	201 (46.6)	98 (22.7)
rs2716191	*MAPKK6*	C/T	SR	341 (73.3)	116 (24.9)	8 (1.7)	149 (72)	54 (26.1)	4 (1.9)
			NR	457 (78.3)	121 (20.7)	6 (1)	336 (77.8)	91 (21.1)	5 (1.2)
rs2715812	*MAPKK6*	C/T	SR	229 (49)	191 (40.9)	47 (10.1)	106 (51)	83 (39.9)	19 (9.1)
			NR	255 (43.6)	266 (45.5)	64 (10.9)	180 (41.7)	199 (46.1)	53 (12.3)
rs11869073	*MAPKK6*	A/C	SR	379 (81)	81 (17.3)	8 (1.7)	170 (81.7)	35 (16.8)	3 (1.4)
			NR	480 (81.8)	104 (17.7)	3 (0.5)	369 (85)	63 (14.5)	2 (0.5)
rs12945375	*MAPKK6*	A/G	SR	386 (82.7)	74 (15.8)	7 (1.5)	173 (83.6)	31 (15)	3 (1.4)
			NR	488 (83.1)	97 (16.5)	2 (0.3)	374 (86.2)	60 (13.8)	0 (0)
rs12939509	*MAPKK6*	A/G	SR	422 (90.2)	44 (9.4)	2 (0.4)	186 (89.4)	21 (10.1)	1 (0.5)
			NR	518 (88.2)	67 (11.4)	2 (0.3)	383 (88.2)	49 (11.3)	2 (0.5)
rs8082399	*MAPKK6*	G/A	SR	382 (81.8)	83 (17.8)	2 (0.4)	166 (79.8)	40 (19.2)	2 (1)
			NR	499 (85.4)	82 (14)	3 (0.5)	371 (86.1)	57 (13.2)	3 (0.7)
rs2716195	*MAPKK6*	G/A	SR	315 (67.7)	141 (30.3)	9 (1.9)	141 (68.4)	61 (29.6)	4 (1.9)
			NR	402 (68.7)	165 (28.2)	18 (3.1)	296 (68.5)	120 (27.8)	16 (3.7)
rs2716223	*MAPKK6*	G/A	SR	129 (27.7)	230 (49.4)	107 (23)	54 (26)	100 (48.1)	54 (26)
			NR	155 (26.5)	279 (47.7)	151 (25.8)	104 (24.1)	209 (48.4)	119 (27.5)
rs2715810	*MAPKK6*	G/A	SR	118 (25.3)	237 (50.7)	112 (24)	51 (24.6)	105 (50.7)	51 (24.6)
			NR	147 (25.1)	287 (49.1)	151 (25.8)	106 (24.5)	210 (48.6)	116 (26.9)
rs7213686	*MAPKK6*	T/C	SR	415 (88.9)	50 (10.7)	2 (0.4)	185 (89.4)	21 (10.1)	1 (0.5)
			NR	516 (87.9)	69 (11.8)	2 (0.3)	381 (87.8)	51 (11.8)	2 (0.5)

Supplementary Table 2. (Continued)

SNP	Gene	Alleles (1/2)	Group	All patients with HCV infection: No. of genotypes (%) 1/1	1/2	2/2	Patients with HCV genotype 1b: No. of genotypes (%) 1/1	1/2	2/2
rs8067307	*MAPKK6*	C/A	SR	310 (66.4)	144 (30.8)	13 (2.8)	134 (64.7)	68 (32.9)	5 (2.4)
			NR	370 (63.1)	197 (33.6)	19 (3.2)	285 (65.7)	135 (31.1)	14 (3.2)
rs4968859	*MAPKK6*	A/C	SR	312 (67)	128 (27.5)	26 (5.6)	136 (65.4)	60 (28.8)	12 (5.8)
			NR	364 (62.2)	194 (33.2)	27 (4.6)	269 (62.3)	140 (32.4)	23 (5.3)
rs9893349	*MAPKK6*	G/A	SR	136 (29.3)	233 (50.2)	95 (20.5)	63 (30.6)	94 (45.6)	49 (23.8)
			NR	154 (26.3)	312 (53.2)	120 (20.5)	116 (26.8)	228 (52.7)	89 (20.6)
rs17690015	*MAPKK6*	G/A	SR	386 (82.7)	78 (16.7)	3 (0.6)	180 (87)	27 (13)	0 (0)
			NR	475 (81.2)	104 (17.8)	6 (1)	362 (83.8)	67 (15.5)	3 (0.7)
rs2715834	*MAPKK6*	G/C	SR	128 (27.4)	239 (51.2)	100 (21.4)	50 (24)	113 (54.3)	45 (21.6)
			NR	148 (25.3)	299 (51)	139 (23.7)	112 (25.9)	217 (50.1)	104 (24)
rs1548444	*MAPKK6*	T/G	SR	216 (46.6)	190 (40.9)	58 (12.5)	100 (48.8)	75 (36.6)	30 (14.6)
			NR	232 (39.8)	286 (49.1)	65 (11.1)	166 (38.6)	210 (48.8)	54 (12.6)
rs2715817	*MAPKK6*	T/C	SR	181 (38.7)	209 (44.7)	78 (16.7)	83 (39.9)	88 (42.3)	37 (17.8)
			NR	226 (38.6)	269 (45.9)	91 (15.5)	170 (39.3)	201 (46.4)	62 (14.3)
rs2715832	*MAPKK6*	T/C	SR	276 (59.2)	162 (34.8)	28 (6)	103 (49.8)	86 (41.5)	18 (8.7)
			NR	312 (53.4)	231 (39.6)	41 (7)	223 (51.7)	179 (41.5)	29 (6.7)
rs7761118	p38 MAP kinase	G/A	SR	398 (85.2)	67 (14.3)	2 (0.4)	175 (84.1)	32 (15.4)	1 (0.5)
			NR	494 (84.6)	86 (14.7)	4 (0.7)	366 (84.7)	64 (14.8)	2 (0.5)
rs2145362	p38 MAP kinase	C/G	SR	142 (30.5)	238 (51.2)	85 (18.3)	57 (27.5)	114 (55.1)	36 (17.4)
			NR	193 (32.9)	281 (48)	112 (19.1)	143 (33)	205 (47.3)	85 (19.6)
rs3752525	p38 MAP kinase	G/T	SR	254 (54.3)	192 (41)	22 (4.7)	107 (51.4)	89 (42.8)	12 (5.8)
			NR	319 (54.3)	226 (38.5)	42 (7.2)	233 (53.7)	169 (38.9)	32 (7.4)
rs3730326	p38 MAP kinase	G/T	SR	433 (92.5)	31 (6.6)	4 (0.9)	191 (91.8)	15 (7.2)	2 (1)
			NR	543 (92.7)	42 (7.2)	1 (0.2)	403 (93.1)	30 (6.9)	0 (0)
rs7770710	p38 MAP kinase	C/T	SR	418 (89.5)	49 (10.5)	0 (0)	190 (91.3)	18 (8.7)	0 (0)
			NR	544 (92.8)	40 (6.8)	2 (0.3)	398 (91.9)	35 (8.1)	0 (0)
rs16884694	p38 MAP kinase	G/A	SR	354 (76)	107 (23)	5 (1.1)	161 (77.4)	46 (22.1)	1 (0.5)
			NR	453 (77.8)	120 (20.6)	9 (1.5)	334 (77.7)	91 (21.2)	5 (1.2)
rs13196204	p38 MAP kinase	T/G	SR	293 (63)	164 (35.3)	8 (1.7)	122 (58.9)	81 (39.1)	4 (1.9)
			NR	387 (66.6)	170 (29.3)	24 (4.1)	282 (65.4)	132 (30.6)	17 (3.9)
rs3804453	p38 MAP kinase	A/G	SR	401 (85.9)	65 (13.9)	1 (0.2)	181 (87)	27 (13)	0 (0)
			NR	508 (86.8)	71 (12.1)	6 (1)	369 (85.4)	60 (13.9)	3 (0.7)
rs3804454	p38 MAP kinase	T/G	SR	364 (77.9)	93 (19.9)	10 (2.1)	162 (77.9)	39 (18.8)	7 (3.4)
			NR	451 (77.2)	124 (21.2)	9 (1.5)	338 (78.2)	89 (20.6)	5 (1.2)
rs10807156	p38 MAP kinase	A/T	SR	164 (35)	235 (50.2)	69 (14.7)	66 (31.7)	115 (55.3)	27 (13)
			NR	217 (37.3)	271 (46.6)	94 (16.2)	159 (36.7)	202 (46.7)	72 (16.6)
rs4844550	*MAPKAPK2*	A/G	SR	228 (49.1)	195 (42)	41 (8.8)	103 (49.5)	85 (40.9)	20 (9.6)
			NR	292 (50)	241 (41.3)	51 (8.7)	211 (49)	174 (40.4)	46 (10.7)
rs10863784	*MAPKAPK2*	C/G	SR	135 (29.2)	224 (48.4)	104 (22.5)	62 (30.4)	96 (47.1)	46 (22.5)
			NR	161 (27.4)	293 (49.9)	133 (22.7)	113 (26)	217 (50)	104 (24)
rs12028997	*MAPKAPK2*	C/T	SR	400 (85.5)	66 (14.1)	2 (0.4)	177 (85.1)	31 (14.9)	0 (0)
			NR	501 (85.5)	80 (13.7)	5 (0.9)	374 (86.4)	55 (12.7)	4 (0.9)
rs4073250	*MAPKAPK2*	C/T	SR	394 (84.9)	68 (14.7)	2 (0.4)	181 (87.9)	25 (12.1)	0 (0)
			NR	492 (84.4)	87 (14.9)	4 (0.7)	360 (83.7)	66 (15.3)	4 (0.9)
rs4072677	*MAPKAPK2*	T/G	SR	186 (39.9)	218 (46.8)	62 (13.3)	83 (40.1)	94 (45.4)	30 (14.5)
			NR	224 (38.2)	288 (49.1)	75 (12.8)	162 (37.3)	211 (48.6)	61 (14.1)
rs12060808	*MAPKAPK2*	C/T	SR	382 (81.8)	77 (16.5)	8 (1.7)	175 (84.5)	28 (13.5)	4 (1.9)
			NR	473 (81)	103 (17.6)	8 (1.4)	347 (80.5)	78 (18.1)	6 (1.4)
rs616589	*MAPKAPK3*	G/A	SR	215 (46)	205 (43.9)	47 (10.1)	111 (53.4)	84 (40.4)	13 (6.3)
			NR	235 (40.3)	271 (46.5)	77 (13.2)	164 (38)	209 (48.4)	59 (13.7)
rs3792323	*MAPKAPK3*	A/T	SR	242 (51.8)	187 (40)	38 (8.1)	124 (59.6)	75 (36.1)	9 (4.3)
			NR	273 (46.7)	253 (43.3)	58 (9.9)	189 (43.9)	196 (45.5)	46 (10.7)
rs3804628	*MAPKAPK3*	G/A	SR	416 (89.3)	48 (10.3)	2 (0.4)	184 (88.5)	22 (10.6)	2 (1)
			NR	519 (88.4)	66 (11.2)	2 (0.3)	389 (89.6)	43 (9.9)	2 (0.5)
rs2040397	*MAPKAPK3*	C/T	SR	288 (61.8)	155 (33.3)	23 (4.9)	124 (59.9)	74 (35.7)	9 (4.3)
			NR	393 (67)	170 (29)	24 (4.1)	282 (65)	132 (30.4)	20 (4.6)

NOTE. Genotype data are presented as the number of subjects with percentages in parentheses. Allele 1, major allele; Allele 2, minor allele.

Hepatology Research 2009; 39: 134–142 doi: 10.1111/j.1872-034X.2008.00416.x

Original Article

FDG positron emission tomography/computed tomography for the detection of extrahepatic metastases from hepatocellular carcinoma

Tomokazu Kawaoka,[1] Hiroshi Aikata,[1] Shintaro Takaki,[1] Kiminori Uka,[1] Takahiro Azakami,[1] Hiromi Saneto,[1] Soo Cheol Jeong,[1] Yoshiiku Kawakami,[1] Shoichi Takahashi,[1] Naoyuki Toyota,[2] Katsuhide Ito,[2] Yutaka Hirokawa[3] and Kazuaki Chayama[1]

[1]*Department of Medicine and Molecular Science, Division of Frontier Medical Science, Programs for Biomedical Research, Graduate School of Biomedical Sciences,* [2]*Department of Radiology, Hiroshima University and* [3]*Department of Radiology, Hiroshima Heiwa Clinic, Hiroshima, Japan*

Aims: To compare the efficacy of positron emission tomography (PET) computed tomography (CT), multi-detector helical computed tomography (MDCT) and bone scintigraphy for the detection of extrahepatic metastases in patients with hepatocellular carcinoma (HCC).

Methods: Thirty-four patients diagnosed with metastatic HCC were enrolled in this study. The lesions included lung ($n = 18$), bone ($n = 12$) and lymph node ($n = 16$) metastases. For receiver operating characteristic (ROC) analysis, lesions were diagnosed as metastatic HCC by two experienced abdominal radiologists. Another three physicians independently reviewed both positive and negative images. Each physician read three sets of images of MDCT, PET–CT and bone scintigraphy for bone metastasis.

Results: The mean sensitivity and specificity for diagnosis of lung metastasis were 85.2 and 88.9% for MDCT, and 59.2 and 92.6% for PET–CT, respectively. For lymph node metastasis, these values were 62.5 and 79.2% for MDCT, and 66.7 and 91.7% for PET–CT, respectively; and for bone metastasis 41.6 and 94.5% for MDCT, 83.3 and 86.1% for PET–CT, and 52.7 and 83.3% for bone scintigraphy, respectively. The mean Az values were 0.95 and 0.77 for MDCT and PET–CT in lung metastasis, respectively, 0.75 and 0.80 for MDCT and PET–CT for lymph node metastasis, respectively, and 0.59, 0.88 and 0.62 for MDCT, PET–CT and bone scintigraphy for bone metastasis, respectively.

Conclusion: PET–CT has high sensitivity and is more suitable for the detection of bone metastases from primary HCC, relative to MDCT and bone scintigraphy.

Key words: ^{18}F-FDG PET–CT, extrahepatic metastases from hepatocellular carcinoma, MDCT, ROC analysis, bone scintigraphy

INTRODUCTION

HEPATOCELLULAR CARCINOMA (HCC) is one of the most common cancers worldwide.[1] Since patients with HCC now live longer than before, thanks to improvements in diagnostic and therapeutic modalities, the number of patients with remote HCC metastases are increasing.[2] Various imaging techniques such as abdominal ultrasonography, multi-detector helical computed tomography (MDCT), computed tomography arterial portography (CTAP), CT during hepatic arteriography (CTHA) and magnetic resonance imaging (MRI) are useful tools for the detection and diagnosis of HCC.[3,4] MDCT, in contrast, is used as a tool for the detection of extrahepatic metastasis.[5] However, these imaging modalities fail to identify metastatic lesions in some patients.

^{18}F-fluoro-2-deoxy-D-glucose (^{18}F-FDG) positron emission tomography (PET) is a well-established, non-invasive diagnostic tool for the detection of a variety of malignant tumors such as neck, lung, pancreas and colon tumors.[6–8] However, ^{18}F-FDG PET is less suitable for the detection of primary HCC because of the variable ^{18}F-FDG uptake in HCC.[8] Nevertheless, a number of studies have used PET–CT for the detection of

Corresponding: Dr Hiroshi Aikata, Department of Medicine and Molecular Science, Division of Frontier Medical Science, Programs for Biomedical Research, Graduate School of Biomedical Sciences, Hiroshima University, 1-2-3 Kasumi, Minami-ku, Hiroshima 734-8551, Japan. Email: aikata@hiroshima-u.ac.jp
Received 14 May 2008; revision 8 July 2008; accepted 21 July 2008.

extrahepatic metastasis and reported its usefulness for this purpose.[9–11] To our knowledge, there are no studies that evaluated PET–CT for the diagnosis of extrahepatic metastases, especially using receiver operating characteristic (ROC) analysis. The multiple-reader ROC study design has become a frequently used tool in diagnostic radiology. With this tool, the investigator can characterize and compare the accuracy of diagnostic tests that rely on subjective interpretation.[12] The aims of the present study were to compare the efficacy of PET–CT as a tool for the detection of metastatic HCCs with MDCT by ROC analysis. For this purpose, we compared the Az value, sensitivity, specificity and positive predictive value of the MDCT and PET–CT for lung, lymph node and bone metastases originating from the liver.

METHODS

Patient population

^{18}F-FDG PET–CT AND MDCT were conducted in 34 consecutive patients diagnosed with extrahepatic metastases based on changes in size and changes in tumor marker between March 2005 and March 2007. In limited cases of bone metastases, bone scintigraphy was also conducted. These patients were enrolled as subjects of this study. Table 1 lists the patients' characteristics and location of extrahepatic metastases.

The primary tumor stage was evaluated according to the criteria of the Liver Cancer Study Group of Japan.[13] The sites of extrahepatic metastases were the lungs in 12 patients, lymph nodes in seven, bones in four, lungs and lymph nodes in three, lymph nodes and bones in five, lungs and bones in two and lungs, lymph nodes and bones in one patient. The total number of extrahepatic metastases was 18 in the lungs, 16 in lymph nodes and 12 in bones. Extrahepatic metastases were also detected in the adrenals in two patients, but these were not investigated due to the small number. There were no metastatic lesions in other organs.

Before performing PET–CT, the purpose of the diagnostic imaging was explained to each patient and written informed consent was obtained. The ethics committee did not require approval or informed consent for this retrospective study, which complied with the principles of the Helsinki Declaration.

Imaging methods

All examinations were performed within a 4-week interval.

Table 1 Characteristics of 34 patients with extrahepatic metastases

Age (years)*	59 (32–80)
Sex (male/female)	28/6
Etiology (HCV/HBV/HCV+HBV/others)	19/11/1/3
Intrahepatic tumor stage (T1/2/3/4)†	7/4/6/17
Child–Pugh score (A/B/C)	26/7/1
α-fetoprotein (ng/mL)*	904 (5–538 100)
Des-γ-carboxy prothrombin (mAU/mL)*	228 (12–645 250)
Site of extrahepatic metastases ($n = 34$)	
Lung/lymph/bone	12/7/4
Lung and lymph/lymph and bone/lung and bone	3/5/2
Lung and lymph and bone	1
Total number of extrahepatic metastases (lung/lymph/bone)	18/16/12
Size of extrahepatic metastases* (mm)	
Lung	9 (4–48)
Lymph	22 (12–87)
Bone	19 (5–120)

*Values are median (range).
†Based on the following three conditions (T factor): solitary, <2 cm in diameter, and no vessel invasion. T1 was defined as fulfilling the three conditions, T2 as fulfilling two of the three conditions, T3 as fulfilling one of the three conditions, T4 as fulfilling none of the three conditions.
HBV, hepatitis B virus; HCV, hepatitis C virus.

MDCT studies

MDCT involved scanning the patients from at least the base of the skull through to the pelvis. CT was first performed without a contrast medium to identify the liver. Using a DUAL SHOT power injector (Nemoto, Tokyo, Japan), 100 mL of iopamidol 300 (Iopamiron 300; Schering, Berlin, Germany) was injected at a rate of 3.5 mL/s through a 22-gauge catheter inserted into the antecubital vein. Four sets of images were acquired in a craniocaudal direction at 20, 40, 65 and 180 s after initiation of contrast medium injection. The first and second acquisitions were used for hepatic arterial phase images, the third acquisition for portal venous phase images, and the fourth acquisition for hepatic venous phase images. The third set of images was obtained during 20-s breath-holding, while those of the other acquisitions were achieved during 10-s breath-holding. All scans were performed on a LightSpeed Ultra 16 CT scanner (General Electric Medical Systems, Milwaukee, WI, USA) with scan parameters including 0.9-s gantry rotation speed, scan mode (20 mm Beam, Helical pitch 1.375), 1.25-mm slice thickness, 27.5 mm per rotation

table speed and reconstruction intervals of 0.625 mm for portal venous phase images.

^{18}F-FDG PET–CT studies

All PET scans were performed on a combined PET–CT system (Discovery ST; General Electric Medical Systems). The ^{18}F-fluoride was produced by an on-site cyclotron (HM12; Sumitomo Heavy Industry, Tokyo, Japan). ^{18}F-FDG was synthesized by the automated Hamacher method and tested for sterility, pyrogenicity and radiochemical purity on each production run. All patients were fasted for at least 5 h before injection of 300–400MBq ^{18}F-FDG. Imaging commenced 1 h after injection. Scanning included the area from at least the base of the skull through to the femoral region, applying a three-dimensional mode with a 1.5 min acquisition per bed position. All studies were reconstructed using default vender-implemented iterative reconstruction algorithm.

Bone scintigraphy studies

For bone scintigraphy, technetium-99m methylene diphosphonate was injected at a dose of 555 MBq (^{15m}Ci)-740 MBq (^{20m}Ci), and imaging begun 2 h after injection. Examinations were performed with a large-field-of-view gamma camera, with a high-resolution collimator. Multiple overlapping spot images were obtained of the entire body.

Image analysis

The obtained images were analyzed before the pathologic results became known, and were presented in a random order. Before performing ROC analysis, two experienced radiologists (Y. H., K. I.), who served as the study coordinators in the ROC analysis, defined the gold standard. They were given the images obtained from the above imaging modalities, including MDCT, ^{18}F-FDG PET–CT and bone scintigraphy, as well as the operative, laboratory and histological findings. They defined the gold standard by the appearance of mass lesion from those not detected previously, worsening of HCC, increase in tumor size, increase in tumor marker and histological finding.

Ten patients later underwent autopsy and two patients underwent surgery for lung tumor. Another group of three gastroenterologists (H. A., K. U., S. T) with a specialty in imaging diagnosis who had at least 10 years' experience in interpreting MDCT and bone scintigraphy and 3 years' experience in interpreting ^{18}F-FDG PET–CT images in their practices, independently reviewed the three sets of images (MDCT, fusion images of ^{18}F-FDG PET–CT and bone scintigraphy). The databases of all images were also used as the reference libraries (online atlases) for our intelligent workstation.

These gastroenterologists were informed that the patients had HCCs and had been referred for pretherapeutic assessment of suspected metastasis, but knew nothing else about the patients. To minimize learning bias, the reviewing order was randomized and the reviewing procedure was conducted in four sessions at 2-week intervals. Three gastroenterologists, one for each modality, read the MDCT, fusion images of ^{18}F-FDG PET–CT and bone scintigraphy separately and prospectively at each participating site. In the above analyses, the same numbers of patients that did not have HCC metastasis were included as negative images (lung/lymph/bone = 18/16/12).

On PET–CT images, a region of interest (ROI) was drawn over the areas of maximum intensity in each lesion for semi-quantitative analysis. The ROI data were processed as a standardized uptake value (SUV). Lesions were identified as positive if the accumulation of ^{18}F-FDG was higher than a normal contralateral structure or surrounding tissues. A lack of increased activity was considered a normal finding.

Each reader scored each image for the presence of metastatic HCC lesions and assigned confidence levels to his observation (1 = definitely negative, 2 = probably negative, 3 = possibly positive, 4 = probably positive, 5 = definitely positive).

Statistical analysis

For each imaging technique, a binomial ROC curve was fitted to each observer's confidence rating data by maximum likelihood estimation with a ROC analysis program (ROCKIT 0.9.1B; Metz CE, Chicago, IL, USA).[14] The diagnostic accuracy of each imaging technique was determined by calculating the area (Az) under each observer-specific binomial ROC curve when it was plotted in the designated square. Composite ROC curves representing the performance of all physicians as a single observer were obtained for each pair of imaging sequences using the maximum likelihood curve-fitting algorithm to rate the pooled data of the three independent physicians. A P value less than 0.05 was considered to represent statistically significant difference. The relative sensitivities of each imaging modality for detection by three individual observers and extrahepatic metastases composite data were determined using the number of assigned score of 4 or more for extrahepatic metastases.

Table 2 Az value, sensitivity, specificity and positive predictive value in detection of lung metastasis

Observer	Az value		Sensitivity (%)		Specificity (%)		Positive predictive value (%)	
	MDCT	PET–CT	MDCT	PET–CT	MDCT	PET–CT	MDCT	PET–CT
1	0.956	0.691	88.9	55.6	94.4	94.4	94.1	100.0
2	0.957	0.807	77.8	72.2	94.4	88.9	93.3	100.0
3	0.938	0.814	88.9	50.0	88.9	94.4	88.9	100.0
Mean	0.950	0.771	85.2	59.2	88.9	92.6	92.1	100.0
P value*		0.054		0.128		1.0		0.039

*Compared with the value for MDCT.
MDCT, multi-detector helical computed tomography; PET–CT, positron emission tomography – computed tomography.

The specificity of each imaging modality was determined by the number of assigned score of 3 or less without extrahepatic metastases. The relative sensitivities and specificities of each imaging modality were compared using the McNemar test. To assess inter-observer variability in interpreting images, kappa statistics were used to measure the degree of agreement between observers.[15] A kappa value greater than 0 was considered to indicate a positive correlation. Values up to 0.4 were considered to indicate positive but poor correlation; values of 0.41–0.75, good correlation; and values greater than 0.75, excellent correlation.

RESULTS

Lung metastasis

THREE OBSERVERS ACHIEVED a slightly lower diagnostic performance on PET–CT images than MDCT, but the difference in the mean Az values of both image sets was not significant. The positive predictive value for analysis of MDCT was significantly lower than that of PET–CT for all observers (Table 2, Fig. 1a). False negative lesions in PET–CT were 16.7% (3/18). The PET–CT showed no accumulation of ^{18}F-FDG in both metastatic lesions and in primary lesions of HCC in three cases. The tumor size of these three cases was 3, 5 and 8 mm, respectively. The images of one of these patients are shown in Figure 2.

Lymph node metastasis

There were no significant differences between analyses of MDCT and PET–CT images for all observers in the Az value, sensitivity, specificity and positive predictive values (Table 3, Fig. 1b). False negative lesions in PET–CT were 6.3% (1/16). The PET–CT showed no accumulation of ^{18}F-FDG in both the metastatic lesions and primary lesions of HCC in one case. Figure 3 shows that the lymphadenopathy detected by MDCT was considered to be benign lesion due to no accumulation of ^{18}F-FDG.

Bone metastasis

The Az value and sensitivity were higher on PET–CT images than MDCT (mean Az, 0.883 and 0.594, respectively; $P = 0.027$, mean sensitivity, 83.3 and 41.6%,

Table 3 Az value, sensitivity, specificity and positive predictive value in detection of lymph node metastasis

Observer	Az value		Sensitivity (%)		Specificity (%)		Positive predictive value (%)	
	MDCT	PET–CT	MDCT	PET–CT	MDCT	PET–CT	MDCT	PET–CT
1	0.794	0.824	50.0	62.5	87.5	87.5	80.0	83.3
2	0.683	0.842	50.0	68.8	87.5	93.8	80.0	91.7
3	0.787	0.761	87.5	68.8	62.5	93.8	70.0	100.0
Mean	0.755	0.809	62.5	66.7	79.2	91.7	76.7	91.7
P value*		0.425		0.752		0.335		0.197

*Compared with the value for MDCT.
MDCT, multi-detector helical computed tomography; PET–CT, positron emission tomography – computed tomography.

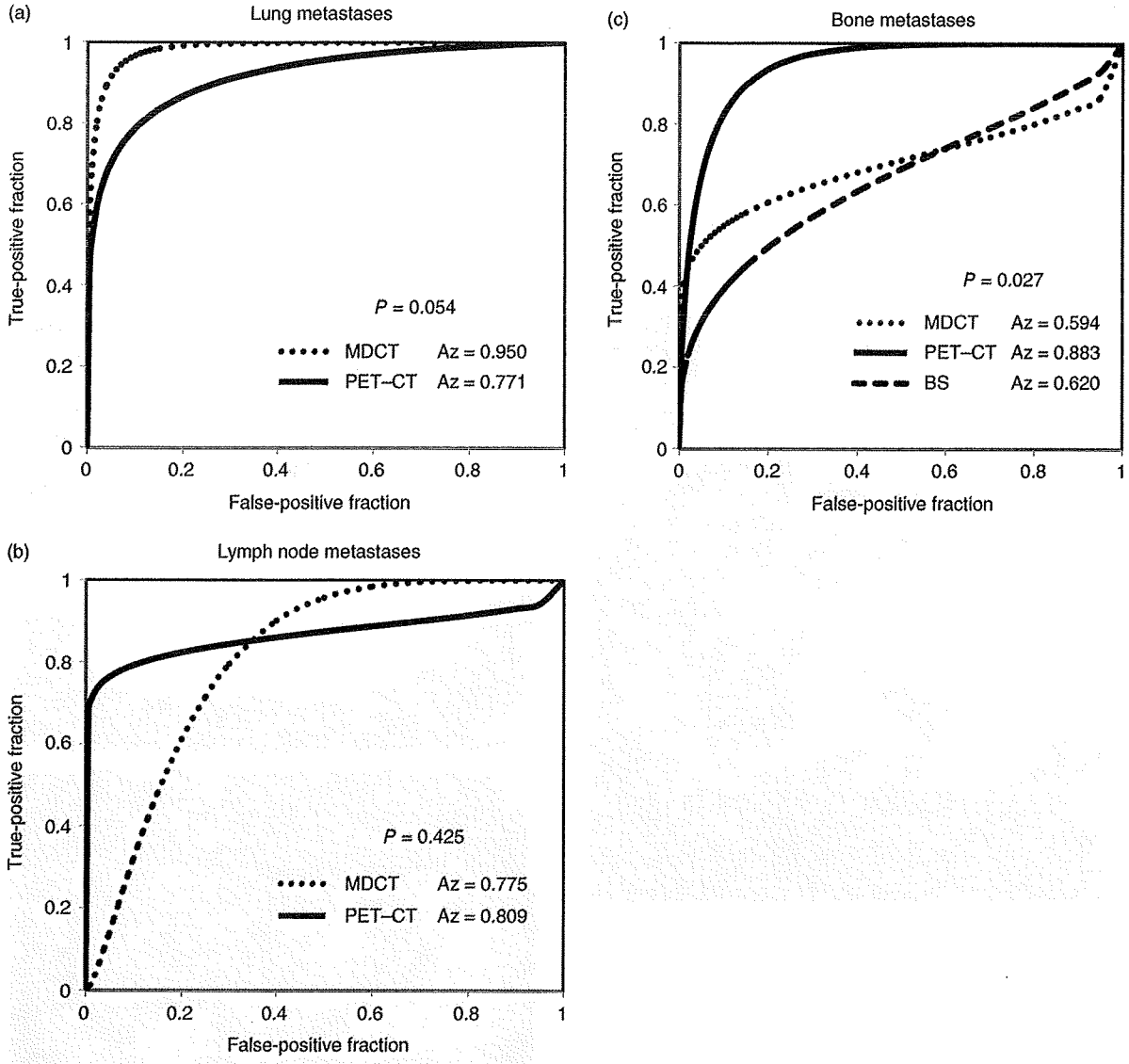

Figure 1 Receiver operating characteristic (ROC) curves for (a) lung metastases, (b) lymph node metastases and (c) bone metastases using data of all observers.

respectively; $P = 0.002$). However, there were no significant differences in specificity and positive predictive value between analysis of MDCT and PET–CT images for all observers. The sensitivity of PET–CT in detecting bone metastases from primary HCC tended to be higher than bone scintigraphy (83.3 and 52.7%, respectively; $P = 0.053$). Furthermore, the Az value of PET–CT was higher than bone scintigraphy (0.883 and 0.620, respectively; $P = 0.027$, Table 4, Fig. 1c).

False negative lesions were 16.7% (2/12) in MDCT and 0% in PET–CT (Fig. 4a,b). These two lesions which could not be detected by MDCT were clearly detected by PET-CT, showed the accumulation of ^{18}F-FDG and were not detected by bone scintigraphy (Fig. 4c).

The mean kappa values were 0.42, 0.45 and 0.52 for lung metastases, lymph node metastases and bone metastasis, respectively. All kappa values were considered to represent good correction.

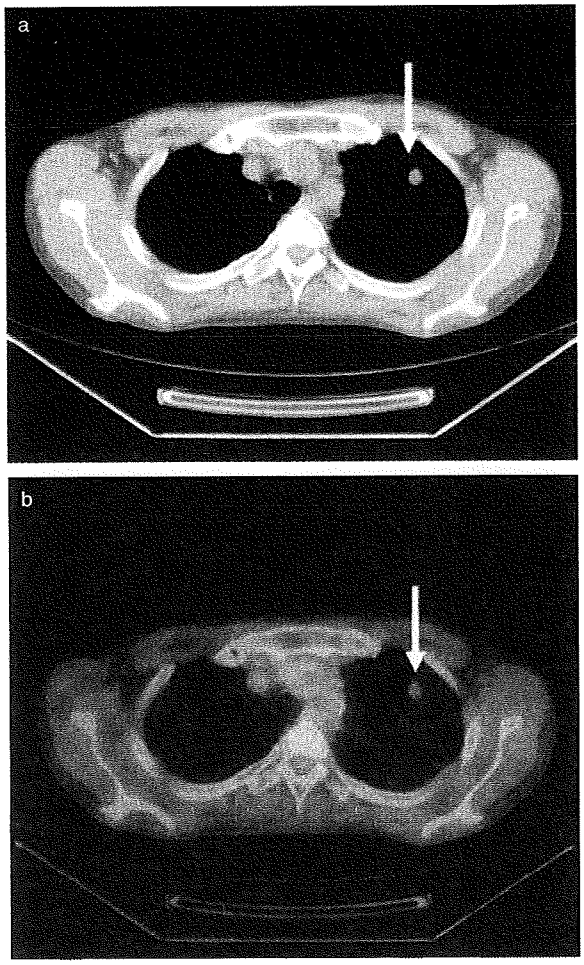

Figure 2 A 50-year-old male patient with hepatocellular carcinoma (HCC). (a) Multi-detector helical computed tomography (MDCT) showed lung metastasis measuring 5 mm in diameter in the left lung (white arrow). (b) The corresponding positron emission tomography – computed tomography (PET–CT) showed no accumulation of 18F-FDG in the left lung lesion.

DISCUSSION

PET IS A new, important imaging technique in the diagnosis of malignancy and has the potential to greatly enhance pre-operative staging of patients with cancer. In fact, PET–CT has been increasingly used for tumor staging.[6–8]

The pathology of extrahepatic metastases from primary HCC is usually moderately differentiated, poorly differentiated, or undifferentiated HCC.[16] PET can detect extrahepatic metastases with high sensitivity, probably due to the relationship between histological grading and *in vitro* enzymatic activity of glucose metabolism. Aerobic glycolysis and glucose metabolism are increased in moderately differentiated, poorly differentiated and undifferentiated hepatoma cells.[17]

Few studies have investigated the relationship between PET–CT and extrahepatic metastases of HCC.

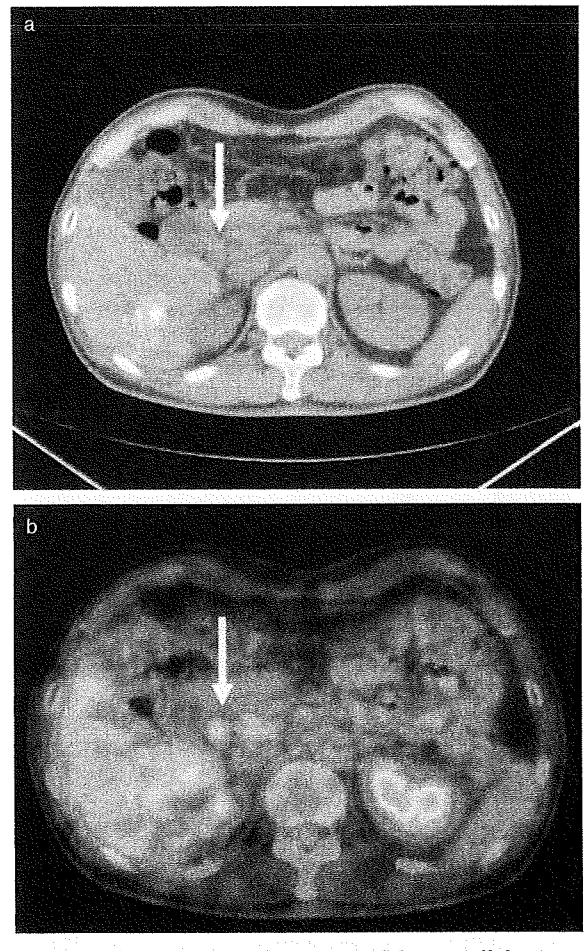

Figure 3 A 62-year-old male patient with hepatocellular carcinoma (HCC). This patient had lymph node swelling measuring 12 mm in diameter in the abdomen (a). The lesion was detected by multi-detector helical computed tomography (MDCT) (white arrow). However, the size of this lesion did not change over a 6-month period and the tumor marker was negative (b). The maximum standardized uptake value (SUV) was 2.7 in positron emission tomography – computed tomography (PET–CT) (white arrow) and this lesion was diagnosed as benign.

Table 4 Az value, sensitivity, specificity and positive predictive value in detection of bone metastasis

Observer	Az value			Sensitivity (%)			Specificity (%)			Positive predictive value (%)		
	MDCT	PET–CT	BS	MDCT	PET–CT	BS	MDCT	PET–CT	BS	MDCT	PET–CT	BS
1	0.640	0.801	0.609	50.0	91.7	50.0	100.0	75.0	83.3	100.0	78.5	71.4
2	0.506	0.884	0.627	41.7	83.3	50.0	91.7	83.3	83.3	83.3	83.3	85.7
3	0.638	0.968	0.625	33.3	75.0	58.3	91.7	100.0	83.3	80.0	100.0	66.7
Mean	0.594	0.883	0.620	41.6	83.3	52.7	94.5	86.1	83.3	87.7	87.3	74.6
P value	0.027*		0.027†	0.002*		0.053†	0.18*		1.0†	0.70*		0.27†

BS, bone scintigraphy; MDCT, multi-detector helical computed tomography; PET–CT, positron emission tomography – computed tomography.
*Compared MDCT with PET-CT.
†Compared BS with PET-CT.

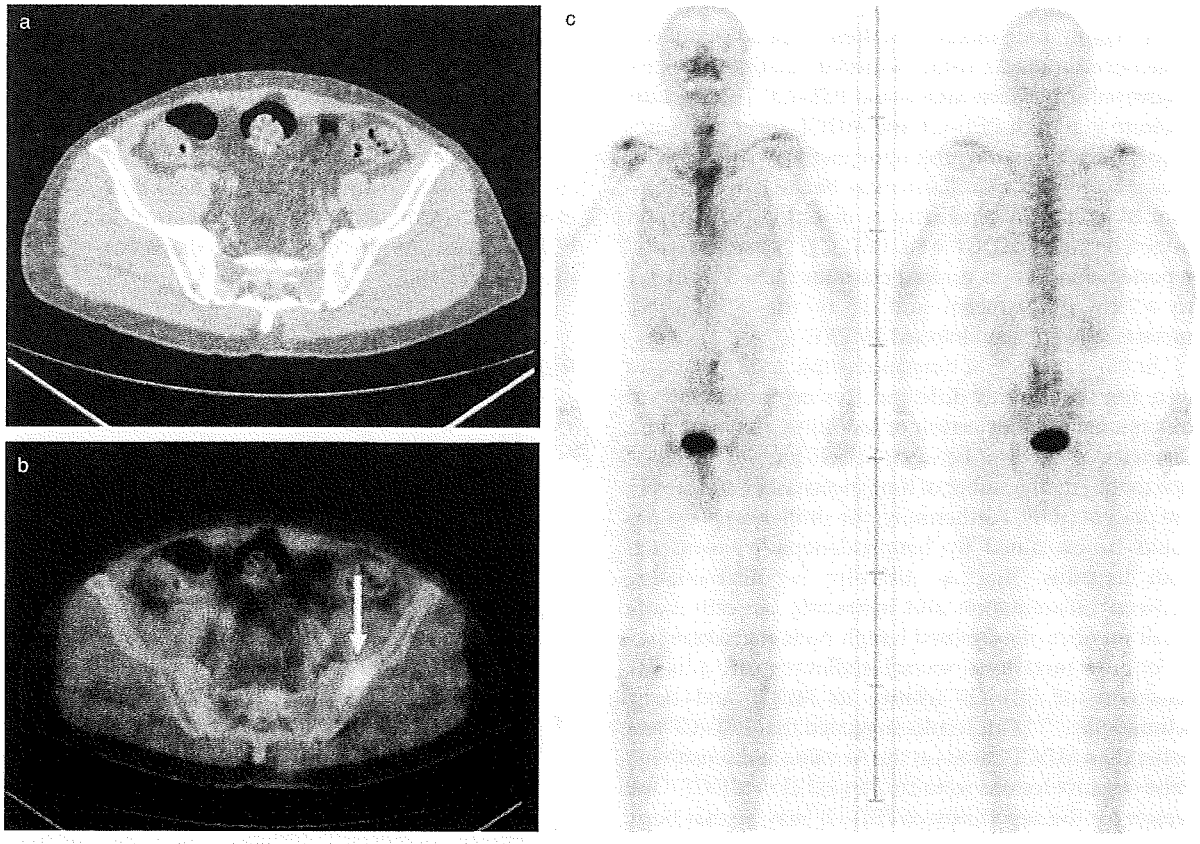

Figure 4 A 76-year-old male patient with hepatocellular carcinoma (HCC). This patient had a bone metastatic lesion measuring 18 mm in diameter in the left iliac bone. (a) The lesion was not detected by multi-detector helical computed tomography (MDCT). (b) The same tumor was clearly detected by positron emission tomography – computed tomography (PET–CT) and showed accumulation of ^{18}F-FDG (SUV = 3.3) (white arrow). (c) The same tumor was not detected by bone scintigraphy.

Sugiyama *et al.*[9] reported a detection rate of 83% for extrahepatic metastases in patients with HCC, including lesions more than 1 cm in diameter. Nagaoka *et al.*[10] also reported that PET alone detected 52 of 58 (89.6%) extrahepatic metastases. However, there are no reports that compared the efficacy of PET–CT as a detection tool for metastatic HCCs with that of MDCT using ROC analysis.

In the present study, the sensitivity of MDCT in the detection of lung metastasis was significantly higher than that of PET–CT, and the Az value of MDCT was significantly higher than that of PET–CT. This is probably mainly due to the higher sensitivity for detection lesions with maximum diameter of ≤10 mm by MDCT than PET–CT. These results are compatible with the findings of Sugiyama *et al.*[9] who suggested that PET–CT is a potentially useful diagnostic tool for the identification of extrahepatic HCC larger than 10 mm. These results indicate that MDCT is a better modality than PET–CT in the detection of lung metastases from HCC.

For lymph node metastases, there were no significant differences in the Az value, sensitivity and positive predictive value between MDCT and PET–CT. These results indicate that both PET–CT and MDCT are equally suitable for detection of lymph node metastases from HCC. One reason for the similarity may be the lack of significant difference in sensitivity of detecting large lymph nodes between MDCT and PET–CT. Nagaoka *et al.*[10] reported that lymph node metastases ranged from 1.3 to 4.7 cm in diameter, and 21 of the 22 (95.4%) metastases were also detected by PET.

The kappa values for lung and lymph node metastases were not significantly different. This is probably due to differences in the detection of lesions with a maximum diameter of ≤10 mm between MDCT and PET–CT and due to the small number of lung metastases examined in the present study. Furthermore, the similar kappa values could be explained by lymphadenopathy associated with hepatitis, that is, difficulty in differentiating between inflammation and metastasis, as well as the small number of examined lymph node metastases.

For bone metastases, several studies reported a higher sensitivity of PET–CT relative to MDCT and bone scintigraphy.[5,9,10] Our results suggested that PET–CT was better than MDCT based on the Az value and sensitivity. False negative lesions were 16.7% (2/12) in MDCT. One reason for the superiority of PET–CT may be that bone metastatic lesions from HCC are more likely to be osteolytic than osteoblastic lesions.[18] It has been documented that PET–CT is more sensitive than bone scintigraphy in detecting osteolytic metastatic lesions from primary cancers of the breast and non-small-cell lung cancer.[19] This difference was attributed to differences in the osteoblastic bone response and glucose uptake by tumor cells.[20] Bone metastasis is painful and reduces the quality of life of patients. Thus, early detection of bone metastasis by PET–CT should allow early treatment of pain by radiotherapy, chemotherapy, radiofrequency ablation therapy, or cementoplasty.[21]

In general, extrahepatic metastases are not limited to a single lesion in a single organ and many patients present with multiple metastases in different organs.[22] Katyal *et al.*[5] reported the presence of multiple metastatic lung lesions in 28% of their patients by MDCT and Yuki *et al.*[23] reported bone metastases in 39 patients (16.3%) of their 240 patients who had HCC at autopsy. When a patient is suspected of having one metastasis by MDCT, we recommend performing PET–CT, since bone metastases are more accurately detected by PET–CT, thus allowing early therapy and perhaps a better prognosis. In fact, 16.7% (2/12) of bone metastases that were not detected by MDCT were clearly detected by PET–CT in our study.

In conclusion, our study compared the detection of extrahepatic metastatic lesions from primary HCC by PET–CT using ROC analysis. PET–CT has high sensitivity and is more suitable for the detection of bone metastases from primary HCC, relative to MDCT. PET–CT may be effective for the diagnosis of bone metastases.

REFERENCES

1 El-Serag HB, Mason AC. Rising incidence of hepatocellular carcinoma in the United States. *N Engl J Med* 1999; 340: 745–50.
2 Poon RT, Fan ST, Lo CM *et al.* Improving survival results after resection of hepatocellular carcinoma: a prospective study of 377 patients over 10 years. *Ann Surg* 2001; 234: 63–70.
3 Kim SR, Ando K, Mita K *et al.* Superiority of CT arterioportal angiography to contrast-enhanced CT and MRI in the diagnosis of hepatocellular carcinoma in nodules smaller than 2 cm. *Oncology* 2007; 72 (Suppl 1): 58–66.
4 Matsui O, Kadoya M, Suzuki M *et al.* Work in progress: dynamic sequential computed tomography during arterial portography in the detection of hepatic neoplasms. *Radiology* 1983; 146: 721–7.
5 Katyal S, Oliver JH 3rd, Peterson MS, Ferris JV, Carr BS, Baron RL. Extrahepatic metastases of hepatocellular carcinoma. *Radiology* 2000; 216: 698–703.
6 Rigo P, Paulus P, Kaschten B J *et al.* Oncological application of positron emission tomography with

fluorine-18 fluorodeoxyglucose. *Eur J Nucl Med* 1996; 23: 1641–74.
7 Giannopoulou C. The role of SPECT and PET in monitoring tumor response to therapy. *Eur J Nucl Med Mol Imaging* 2003; 30: 1173–200.
8 Böhm B, Voth M, Geoghegan J. *et al.* Impact of positron emission tomography on strategy in liver resection for primary and secondary liver tumors. *J Cancer Res Clin Oncol* 2004; 130: 266–72.
9 Sugiyama M, Sakahara H, Torizuka T *et al.* 18F-FDG PET in the detection of extrahepatic metastases from hepatocellular carcinoma. *J Gastroenterol* 2004; 39: 961–8.
10 Nagaoka S, Itano S, Ishibashi M *et al.* Value of fusing PET plus CT images in hepatocellular carcinoma and combined hepatocellular and cholangiocarcinoma patients with extrahepatic metastases: preliminary findings. *Liver Int* 2006; 26: 781–8.
11 Yoon KT, Kim JK, Kim DY *et al.* Role of 18F-Fluorodeoxyglucose positron emission tomography in detecting extrahepatic metastases in pretreatment staging of hepatocellular carcinoma. *Oncology* 2007; 72 (Suppl 1): 104–10.
12 Obuchowski NA. New methodological tools for multiple-reader ROC studies. *Radiology* 2007; 243: 10–12.
13 Liver Cancer Study Group of Japan. The General Rules for the Clinical and Pathological Study of Primary Liver Cancer (in Japanese), 4th edn, Tokyo: Kanehara, 2000.
14 Metz CE. ROC methodology in radiological imaging. *Invest Radiol* 1986; 21: 720–33.
15 Koch GG, Landia JR, Freeman JL, Freeman DH Jr, Lehnen RC. A general methodology for the analysis of experiments with repeated measurement of categorical data. *Biometrics* 1977; 33: 133–58.
16 Kaczynski J, Hansson G, Wallerstedt S. Metastases in cases with hepatocellular carcinoma in relation to clinicopathologic features of the tumor. An autopsy study from a low endemic area. *Acta Oncol* 1995; 34: 43–8.
17 Torizuka T, Tamaki N, Inokuma T *et al.* In vivo assessment of glucose metabolism in hepatocellular carcinoma with FDG-PET. *J Nucl Med* 1995; 36: 1811–17.
18 Schirrmeister H, Guhlmann A, Elsner K *et al.* Sensitivity in detecting osseous lesions depends on anatomic localization: planar bone scintigraphy versus 18F PET. *J Nucl Med* 1999; 40: 1623–9.
19 Bradley JD, Dehdashti F, Muntun MA, Ramaswamy G, Trinkaus K Siegel BA. Positron emission tomography in limited-stage small-cell lung cancer: a prospective study. *J Clin Oncol* 2004; 22: 3248–54.
20 Cook GJ, Houston S, Rubens R, Maisey MN, Fogelman I. Detection of bone metastases in breast cancer with FDG-PET. Differing metabolic activity in osteoblastic and osteolytic lesion. *J Clin Oncol* 1998; 16: 3375–9.
21 Kodama H, Aikata H, Uka K *et al.* Efficacy of percutaneous cementoplasty for bone metastasis from hepatocellular carcinoma. *Oncology* 2007; 72: 285–92.
22 Uka K, Aikata H, Takaki S *et al.* Clinical features and prognosis of patients with extrahepatic metastases from hepatocellular carcinoma. *World J Gastroenterol* 2007; 13: 414–20.
23 Yuki K, Hirohashi S, Sakamoto M, Kanai T, Shimosato Y. Growth and spread of hepatocellular carcinoma. A review of 240 consecutive autopsy cases. *Cancer* 1990; 66: 2174–9.

Hepatology Research 2009; 39: 415–420 doi: 10.1111/j.1872-034X.2008.00448.x

Case Report

Successful treatment of pulmonary metastases associated with advanced hepatocellular carcinoma by systemic 5-fluorouracil combined with interferon-α in a hemodialysis patient

Yoshio Katamura, Hiroshi Aikata, Yuki Kimura, Takahiro Azakami, Tomokazu Kawaoka, Shintaro Takaki, Koji Waki, Akira Hiramatsu, Yoshiiku Kawakami, Shoichi Takahashi and Kazuaki Chayama

Department of Medicine and Molecular Science, Division of Frontier Medical Science, Programs for Biomedical Research, Graduate School of Biomedical Sciences, Hiroshima University, Hiroshima, Japan

A 54-year-old man maintained on hemodialysis had a relapse of multiple pulmonary metastases after multimodal therapy for primary hepatocellular carcinoma (HCC). He was treated with tegafur-uracil (UFT; 400 mg/day) and interferon alfa (IFN-α; 5×10^6 units three times per week) for 4 weeks. Following this he was treated with systemic 5-fluorouracil (5-FU; 1000 mg/day, 5 days per week) and cisplatin (CDDP; 10 mg/day, 5 days per week for 2 weeks). The response to the above treatments was inadequate; pulmonary metastasis deteriorated. Finally, we selected systemic chemotherapy of 5-FU (750 mg/day, 5 days per week) and recombinant IFN-α-2b (3×10^6 units three times per week) for 2 weeks. This therapy resulted in excellent shrinkage of pulmonary metastases, without severe adverse reactions. Hemodialysis was performed three times a week. We report a case of successful treatment of pulmonary metastases by systemic combination chemotherapy of 5-FU–IFN, previously unsuccessfully treated with UFT–IFN and 5-FU–CDDP in a patient on hemodialysis. Further studies are needed to select appropriate drugs with fluoropyrimidine-based systemic chemotherapy, and to analyze the pharmacokinetics of those agents in hemodialysis patients with HCC and extrahepatic metastases.

Key words: extrahepatic metastases, 5-fluorouracil, hemodialysis, hepatocellular carcinoma, interferon, pulmonary metastasis, systemic combination chemotherapy

INTRODUCTION

HEPATOCELLULAR CARCINOMA (HCC) is one of the most common cancers and causes of cancer death worldwide.[1] Development of new diagnostic techniques, such as ultrasonography, computed tomography (CT), magnetic resonance imaging, and angiography, and advancements in therapeutic modalities such as surgical resection, radiofrequency ablation (RFA), percutaneous ethanol injection (PEI), transcatheter arterial chemoembolization (TACE), and intra-arterial infusion via implantable drug delivery systems have gradually improved the prognosis of HCC patients. Nevertheless, the prognosis of patients with advanced HCC and extrahepatic metastases is still poor[2–4] and the standard therapeutic modality for HCC with extrahepatic metastases is still not established. Several investigators suggested recently the use of combination systemic chemotherapies of 5-fluorouracil (5-FU) and cisplatin (CDDP) (5-FU/CDDP), 5-FU with mitoxantrone and CDDP, tegafur/uracil (UFT) and interferon (IFN) (UFT/IFN), 5-FU and IFN (5-FU/IFN), for advanced HCC with extrahepatic metastases.[5–8] It is of note that every regimen is based on fluoropyrimidine, and IFN or CDDP is used concomitantly. However, in an individual case, many questions remain unanswered. For example (i) which concomitant drug should been selected? (ii) What is the mechanism of the antitumor effects of the combination chemotherapeutic agents? (iii) When one concomitant drug is not effective, will the other(s) achieve a good response?, and (iv) Should fluoropyrimidine-based combination chemotherapy be

Correspondence: MD Hiroshi Aikata, Department of Medicine and Molecular Science, Division of Frontier Medical Science, Programs for Biomedical Research, Graduate School of Biomedical Sciences, Hiroshima University, 1-2-3 Kasumi, Minami-ku, Hiroshima 734-8551, Japan. Email: aikata@hiroshima-u.ac.jp
Received 10 July 2008; revised 20 August 2008; accepted 21 August 2008.

used in hemodialysis patients? We and other investigators reported the use of the combination chemotherapy of S-1 and IFN (S-1/IFN) for HCC with extrahepatic metastases.[9,10] However, because 50% of 5-chloro-2,4-dihydroxypyridine (CDHP), an inhibitor of dihydropyrimidine dehydrogenase (DPD), is excreted into the urine, S-1 is considered contraindicated for hemodialysis patients.[11]

We report a patient with HCC and pulmonary metastases who was on maintenance hemodialysis. Although the patient did not show a satisfactory response to two fluorouracil-based regimens of systemic combination chemotherapy, an excellent outcome was finally achieved with systemic combination of 5-FU/IFN.

CASE REPORT

A 54-YEAR-OLD man with hepatitis C virus-related chronic hepatitis was admitted to our hospital for HCC in April 2005. He was on hemodialysis three times a week for chronic renal failure. Computed tomography (CT) showed a solitary tumor measuring 5 cm in diameter in the posterior liver segment and a tumor thrombus in the inferior vena cava (IVC). The intrahepatic tumor and tumor thrombus were treated by TACE and radiotherapy (RT) (30 Gy), respectively. Additional TACE was performed twice in July and October 2005. In November 2005, he underwent a posterior segmentectomy and resection of the right hepatic vein.

In April 2006, chest CT scans showed multiple pulmonary metastases (Fig. 1), but abdominal CT scans performed at the same time did not show any tumors in the liver. Laboratory tests showed α-fetoprotein (AFP) 114 ng/mL, AFP-L3 18% and protein induced by vitamin K antigen II (PIVKA-II) 20 mAU/mL. We selected the combination chemotherapy of UFT/IFN. One course of the chemotherapy consisted of oral UFT (400 mg/day for 4 weeks) and subcutaneous injections of IFN-α (5×10^6 units, three times per week for 4 weeks). After three courses, CT showed deterioration of pulmonary metastases in October 2006 (Fig. 2a–d), and tumor markers were elevated (AFP 749 ng/mL, AFP-L3 30% and PIVKA-II 31 mAU/mL). Therefore, we preferred systemic combination chemotherapy of 5-FU/CDDP. We used intravenous 5-FU (1000 mg/day, three times per week for 2 weeks) and intravenous CDDP (10 mg/day, three times per week for 2 weeks) for two courses. Clinical assessment after these two courses showed no severe adverse reactions. Accordingly, 5-FU and CDDP were administered at the same doses (1000 and 10 mg/day, respectively) but increased to 5 days per week for 2 weeks, per course, for another three courses. 5-FU and CDDP were administered at 1000 mg/24 h and 10 mg/h, respectively. Hemodialysis was performed after one hour of administration of CDDP. In June 2007, after completion of the above five courses of 5-FU/CDDP, a repeat CT showed deterioration of pulmonary metastases (Fig. 2e–h), and laboratory tests showed further elevation of tumor markers (AFP 2300 ng/mL, AFP-L3 33% and PIVKA-II 71 mAU/mL). In August 2007, we switched chemotherapy to systemic 5-FU/IFN; one course consisted of daily intravenous 5-FU (750 mg/day, 5 days per week for 2 weeks) and subcutaneous injection of IFN-α-2b (3×10^6 units three times per week for 2 weeks). 5-FU was administrated at 750 mg/24 h. The dose of 750mg/body instead of 1000 mg/day, was selected for 5-FU because at the latter dose, the patient developed NCI-CTC grade 2 anorexia and diarrhea[12]. Concomitantly, the patient received RT (39 Gy) for the pulmonary metastases infiltrating the right pulmonary artery. After three courses, a repeat CT taken in April 2008 showed excellent shrinkage of pulmonary metastases (Fig. 3), and laboratory tests indicated precipitous falls in AFP and PIVKA-II to < 5.0 ng/mL and 14 mAU/mL, respectively (Fig. 4). Chest CT also showed the appearance of pleuritis at right posterior site and right pleural effusion (Fig. 3). These changes probably represented radioactive pleuritis and pleural effusion. However, they were not associated with any symptoms such as chest pain, dyspnea, or

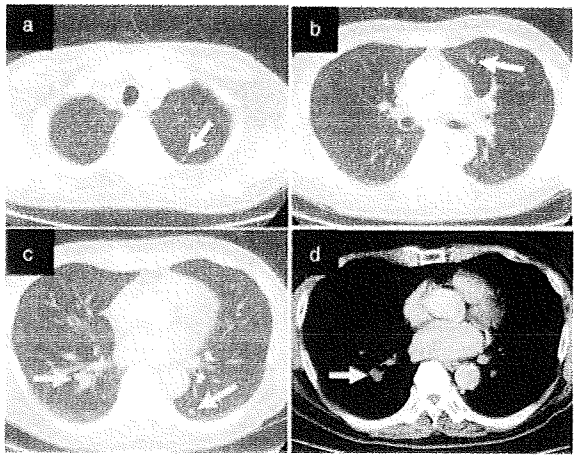

Figure 1 (a–d) Chest computed tomography showed multiple pulmonary metastases in both lung fields (arrows), five months after posterior segmentectomy.

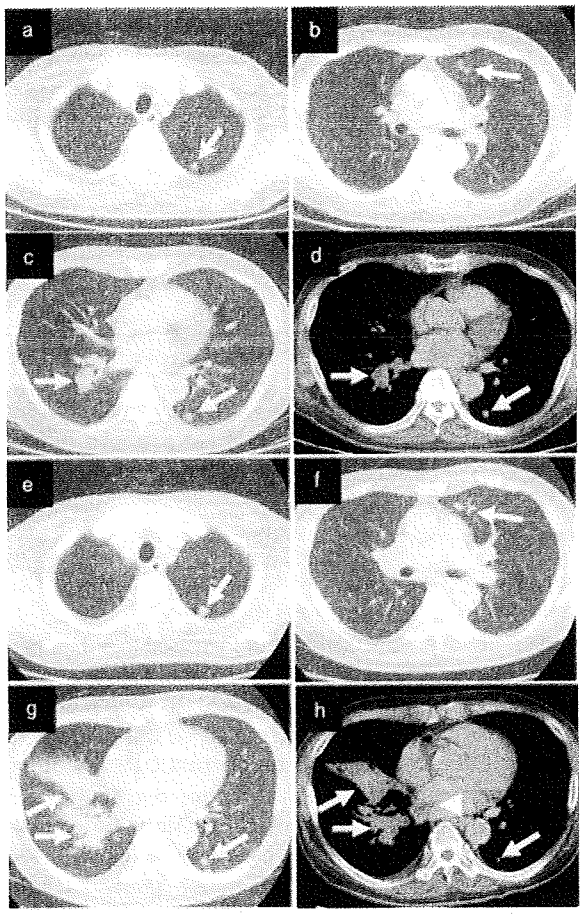

Figure 2 (a–d) Chest computed tomography showed deterioration of pulmonary metastases after three courses of systemic combination chemotherapy of tegafur–uracil and interferon-α (arrows). (e–h) Chest computed tomography showed further deterioration of pulmonary metastases after five courses of systemic combination chemotherapy of 5-fluorouracil and cisplatin (arrows). (h) Pulmonary metastases in the right lung infiltrated the right pulmonary artery (arrowhead).

cough. The adverse reactions to 5-FU/IFN combination chemotherapy included Grade 2–3 anorexia and diarrhea. Laboratory tests showed Grade 4 leukopenia and neutropenia (baseline [before 5-FU/IFN therapy]/lowest; leukocyte count, 2870/980 (/mm^3); neutrophil count 2181/470 (/mm^3); hemoglobin, 8.2/7.7 (g/dL); platelet count, $6.2 \times 10^4/3.5 \times 10^4$ (mm^3), prothrombin activity, 79/70 (%); total bilirubin, 0.3/0.5 (mg/dL); and albumin, 3.5/3.1 (g/dL)). These adverse effects necessitated the administration of granulocyte colony-stimulating factor, but no discontinuation of the chemotherapy since hepatic reserve was preserved. After 5-FU/IFN, the Eastern Cooperative Oncology Group (ECOG) performance status (PS)[13] worsened from 0 to 1 due to Grade 2–3 anorexia and diarrhea, although anorexia and diarrhea disappeared and PS returned to 0 at 2 months after 5-FU–IFN.

DISCUSSION

THERE IS NO standard therapeutic regimen for HCC with extrahepatic metastases. The prognosis of patients with advanced HCC and extrahepatic metastases is still poor.[2–4] Various systemic combination chemotherapies such as UFT–IFN, 5-FU–CDDP, 5-FU–mitoxantrone–CDDP, 5-FU–IFN and S-1–IFN are used.[5–10] With regard to the use of UFT–IFN and 5-FU–CDDP,[5,6] only case reports have been published. One report describes the use of 5-FU–IFN[7] in 7 patients with HCC and distant metastases but does not elaborate on the response rate. Reported response rates are 27% to 5-FU–mitoxantrone–CDDP,[8] and 17 and 25% to S-1–IFN.[9,10] Each of these combination chemotherapies consists of fluoropyrimidine as the key drug, and CDDP or IFN as a concomitant modulator of fluoropyrimidine. To our knowledge, the present case is the first describing the ineffectiveness of 5-FU–CDDP combination

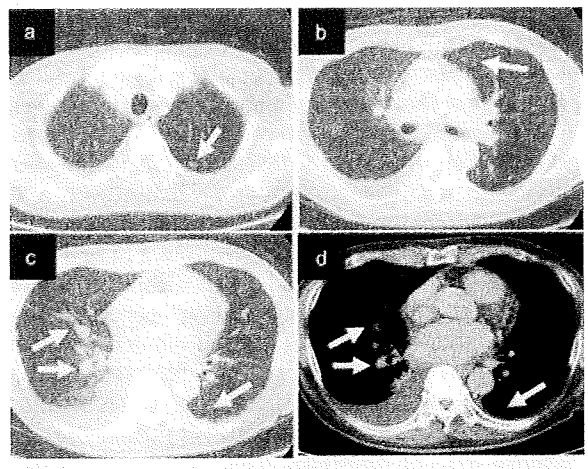

Figure 3 (a–d) Chest computed tomography showed excellent shrinkage of pulmonary metastases after three courses of systemic combination chemotherapy of 5-fluorouracil and interferon-α-2b (arrows). (d) Disappearance of pulmonary metastases infiltrating the right pulmonary artery and appearance of pleuritis at right posterior site with right pleural effusion.

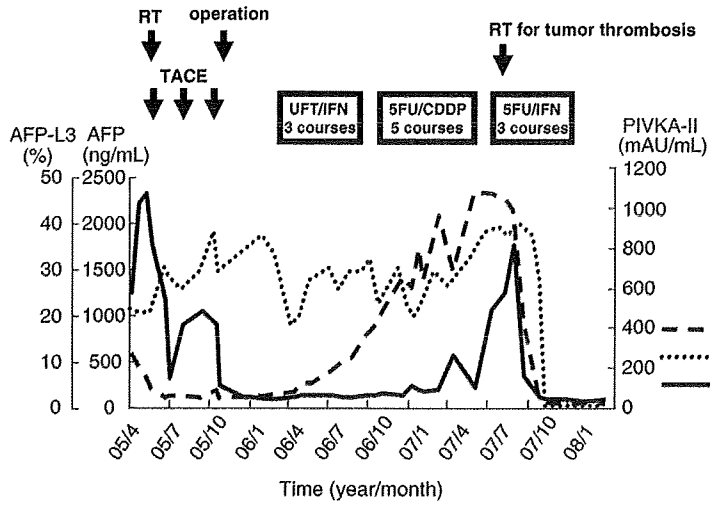

Figure 4 Clinical course. Serum levels of α-fetoprotein (AFP), AFP-L3 and vitamin K antigen II fell precipitously to the normal ranges after systemic combination chemotherapy of 5-fluorouracil and interferon-α-2b and radiotherapy.

therapy, and the effectiveness of 5-FU–IFN for pulmonary metastases associated with primary HCC.

In our hospital, we select systemic combination chemotherapy of S-1–IFN for HCC with extrahepatic metastases if intrahepatic HCC is well controlled.[2,9] As we reported previously, the overall response rate (complete response + partial response) to S-1–IFN is 17%, and the response rate among patients with lung metastases is 21%.[9] With regard to drug metabolism, 53.7% of CDHP, an inhibitor of dihydropyrimidine dehydrogenase, is excreted into the urine,[11] and thus S-1 promotes high plasma concentrations of 5-FU in hemodialysis patients.[14,15] In this regard, the safety of S-1 is yet to be ascertained in hemodialysis patients.

A previous report indicates that although plasma concentrations of 5-FU in hemodialysis patients treated with UFT were about double than in patients with normal renal function on the same combination therapy, no severe adverse reactions were observed in these patients.[16] In addition, because more than 80% of 5-FU is inactivated by DPD, dose modification of intravenously administrated 5-FU for hemodialysis patient is considered unnecessary.[17,18] Based on this background, we selected oral UFT and intravenous 5-FU as one arm of the systemic combination chemotherapy.

Accordingly, we selected UFT–IFN as a first-line therapy. However, when UFT–IFN did not attain clinical efficacy, we speculated that plasma concentrations of 5-FU with oral UFT were inadequate, or IFN was inadequate as a modulator of fluoropyrimidine. Therefore, we tried a systemic combination chemotherapy of 5-FU–CDDP as a second-line therapy. Again, the results of 5-FU–CDDP were unsatisfactory, and thus we selected 5-FU–IFN as the third choice.

In the case reported here, combination chemotherapy of UFT–IFN did not, while that of 5-FU–IFN could attain clinical efficacy. While the exact reason for the different response is not clear at present, we speculate that it is due to therapeutically inadequate plasma concentrations of 5-FU by oral UFT. In our case, we used 10 mg/kg/24 h of 5-FU and 200 mg of UFT twice a day with IFN. We speculate that the former regimen allowed plasma concentration of 5-FU to be higher than the other regimen in the hemodialysis patient. Unfortunately, there is limited information on the pharmacokinetics of 5-FU in hemodialysis patients treated with oral UFT and intravenous 5-FU. Further pharmacokinetic studies are needed to provide safe and effective chemotherapies for hemodialysis patients.

In our patient, the clinical course indicated that while 5-FU/CDDP was ineffective, 5-FU/IFN achieved an excellent outcome. Though both CDDP and IFN play synergistic roles as modulators of fluoropyrimidine, the underlying mechanisms are different. CDDP acts as a modulator by inhibiting intracellular L-methionine metabolism and consequently increases the reduced folate pool such as 5,10-methylenetetrahydrofolate (CH2FH4) and tetrahydrofolate (FH4), which are essential cofactors for the formation of a tight ternary complex of thymidylate synthase (TS) and 5-fluoro-2′-deoxyuridine-5′-monophosphate (FdUMP) derived from 5-FU, resulting in enhancement of its antitumor effects.[19,20] On the other hand, IFN-α acts as a modulator by increasing the level of thymidine phosphorylase,

which is an enzyme responsible for biochemical activation of 5-FU.[21,22] In addition, IFN suppresses cancer cells directly or indirectly via several pathways such as inhibition of cell cycle, boosting p53 activation, and activation of immunocytes.[23–28] With regard to intra-arterial combination chemotherapy for advanced HCC with portal vein tumor thrombosis (PVTT), the response rates to 5-FU–IFN and 5-FU–CDDP seem similar.[29–36] In an individual case, it remains unclear whether 5-FU–CDDP or 5-FUIFN is more effective. Several studies attempted to predict the response to 5-FU–IFN and 5-FU–CDDP chemotherapy. For example, Ota *et al.*[35] reported that the response to 5-FU–IFN combination therapy correlated significantly with the expression level of type I interferon receptor 2 (IFNAR2). Furthermore, Kogure *et al.*[37] reported that the DPD mRNA level could predict the response of human hepatoma cell lines to 5-FU–CDDP. Nishiyama *et al.*[38] indicated that the expression levels of DPD, multidrug resistance-associated protein (MRP), glutathione S-transferase π (GSTπ), and TS gene after exposure to 5-FUCDDP correlated with drug resistance in human gastrointestinal cancer cell lines. Further studies are needed to identify factors that could predict in an individual case the response to 5-FU–CDDP or IFN–5FU and hence help select the most suitable combination chemotherapy.

In our case, the patient received RT for the pulmonary metastases infiltrating the right pulmonary artery concomitantly with 5-FU–IFN. It is possible that this RT also contributed to the fall in tumor markers and shrinkage of tumor at irradiated area. However, the irradiated area was limited to the right pulmonary artery. Thus, we consider that RT did not affect pulmonary metastases other than pulmonary arterial thrombosis.

In conclusion, 5-FU–IFN may be a useful, alternative systemic combination chemotherapy for patients on hemodialysis with HCC and extrahepatic metastases, who do not respond to 5-FU–CDDP.

REFERENCES

1 Parkin DM, Bray F, Ferlay J, Pisani P. Global cancer statistics, 2002. *CA Cancer J Clin* 2005; 55: 74–108.
2 Uka K, Aikata H, Takaki S *et al.* Clinical features and prognosis of patients with extrahepatic metastases from hepatocellular carcinoma. *World J Gastroenterol* 2007; 13: 414–20.
3 Natsuizaka M, Omura T, Akaike T *et al.* Clinical features of hepatocellular carcinoma with extrahepatic metastases. *J Gastroenterol Hepatol* 2005; 20: 1781–7.
4 Okusaka T, Okada S, Ishii H *et al.* Prognosis of hepatocellular carcinoma patients with extrahepatic metastases. *Hepatogastroenterology* 1997; 44: 251–7.
5 Miyamoto A, Umeshita K, Sakon M *et al.* Advanced hepatocellular carcinoma with distant metastases, successfully treated by a combination therapy of alpha-interferon and oral tegafur/uracil. *J Gastroenterol Hepatol* 2000; 15: 1447–51.
6 Anami Y, Oguma S, Matsuda Y *et al.* [Complete disappearance of metastatic lung tumors and mediastinal lymph-node in a case of hepatocellular carcinoma treated by low-dose 5-fluorouracil/CDDP therapy.] *Gan To Kagaku Ryoho* 2005; 32: 1977–80 (in Japanese).
7 Patt YZ, Hassan MM, Lozano RD *et al.* Phase II trial of systemic continuous fluorouracil and subcutaneous recombinant interferon Alfa-2b for treatment of hepatocellular carcinoma. *J Clin Oncol* 2003; 21: 421–7.
8 Ikeda M, Okusaka T, Ueno H, Takezako Y, Morizane C. A phase II trial of continuous infusion of 5-fluorouracil, mitoxantrone, and cisplatin for metastatic hepatocellular carcinoma. *Cancer* 2005; 103: 756–62.
9 Uka K, Aikata H, Mori N *et al.* Combination therapy of oral fluoropyrimidine anticancer drug S-1 and interferon alpha for HCC patients with extrahepatic metastases. *Oncology* 2008; 75: 8–16.
10 Nakamura M, Nagano H, Marubashi S *et al.* Pilot study of combination chemotherapy of S-1, a novel oral DPD inhibitor, and interferon-alpha for advanced hepatocellular carcinoma with extrahepatic metastasis. *Cancer* 2008; 112: 1765–71.
11 Hirata K, Horikoshi N, Aiba K *et al.* Pharmacokinetic study of S-1: a novel oral fluorouracil antitumor drug. *Clin Cancer Res* 1999; 5: 2000–5.
12 NCI Common Toxicity Criteria. http://ctep.cancer.gov/reporting/ctc.html.
13 Oken MM, Creech RH, Tormey DC *et al.* Toxicity and response criteria of the Eastern Cooperative Oncology Group. *Am J Clin Oncol* 1982; 5: 649–55.
14 Tominaga K, Higuchi K, Okazaki H *et al.* Safety and efficacy of S-1, a novel oral fluorouracil anticancer drug, for a chronic renal failure patient maintained on hemodialysis. *Oncology* 2004; 66: 358–64.
15 Tanaka T, Fujita S, Tanaka N, Ooka M, Okajima S, Tanaka N. [TS-1 treatment for progressive gastric cancer in a patient on chronic dialysis – assessment of dosage regimen by monitoring blood concentrations of therapeutic drugs (TDM).] *Gan To Kagaku Ryoho* 2005; 32: 841–5 (in Japanese).
16 Sakamoto K, Arita S, Hisikawa E *et al.* [Pharmacokinetic study of UFT in cancer patients receiving maintenance dialysis.] *Gan To Kagaku Ryoho* 1995; 22: 239–44 (in Japanese).
17 Pinedo HM, Peters GF. Fluorouracil: biochemistry and pharmacology. *J Clin Oncol* 1988; 6: 1653–64.
18 Schilsky RL. Renal and metabolic toxicities of cancer chemotherapy. *Semin Oncol* 1982; 9: 75–83.

19 Scanlon KJ, Newman EM, Lu Y, Priest DG. Biochemical basis for cisplatin and 5-fluorouracil synergism in human ovarian carcinoma cells. *Proc Natl Acad Sci USA* 1986; 83: 8923–5.
20 Shirasaka T, Shimamoto Y, Ohshimo H, Saito H, Fukushima M. Metabolic basis of the synergistic antitumor activities of 5-fluorouracil and cisplatin in rodent tumor models in vivo. *Cancer Chemother Pharmacol* 1993; 32: 167–72.
21 Braybrooke JP, Propper DJ, O'Byrne KJ *et al.* Induction of thymidine phosphorylase as a pharmacodynamic endpoint in patients with advanced carcinoma treated with 5-fluorouracil, folinic acid and interferon alpha. *Br J Cancer* 2000; 83: 219–24.
22 Wadler S, Schwartz EL. Antineoplastic activity of the combination of interferon and cytotoxic agents against experimental and human malignancies: a review. *Cancer Res* 1990; 50: 3473–86.
23 Yano H, Iemura A, Haramaki M *et al.* Interferon alfa receptor expression and growth inhibition by interferon alfa in human liver cancer cell lines. *Hepatology* 1999; 29: 1708–17.
24 Murphy D, Detjen KM, Welzel M, Wiedenmann B, Rosewicz S. Interferon-alpha delays S-phase progression in human hepatocellular carcinoma cells via inhibition of specific cyclin-dependent kinases. *Hepatology* 2001; 33: 346–56.
25 Takaoka A, Hayakawa S, Yanai H *et al.* Integration of interferon-α/β signalling to p53 responses in tumor suppression and antiviral defence. *Nature* 2003; 424: 516–23.
26 Ortaldo JR, Mantovani A, Hobbs D, Rubinstein M, Pestka S, Herberman RB. Effects of several species of human leukocyte interferon on cytotoxic activity of NK cells and monocytes. *Int J Cancer* 1983; 31: 285–9.
27 Brinkmann V, Geiger T, Alkan S, Heusser CH. Interferon alpha increases the frequency of interferon gamma-producing human CD4+ T cells. *J Exp Med* 1993; 178: 1655–63.
28 Uno K, Shimizu S, Ido M *et al.* Direct and indirect effects of interferon on in vivo murine tumor cell growth. *Cancer Res* 1985; 45: 1320–7.
29 Uka K, Aikata H, Takaki S *et al.* Pre-treatment predictor of response, time to progression and survival to intraarterial 5-fluorouracil/interferon combination therapy in patients with advanced hepatocellular carcinoma. *J Gastroenterol* 2007; 42: 845–53.
30 Ando E, Yamashita F, Tanaka M, Tanikawa K. A novel chemotherapy for advanced hepatocellular carcinoma with tumor thrombosis of the main trunk of the portal vein. *Cancer* 1997; 79: 1890–6.
31 Ando E, Tanaka M, Yamashita F *et al.* Hepatic arterial infusion chemotherapy for advanced hepatocellular carcinoma with portal vein tumor thrombosis: analysis of 48 cases. *Cancer* 2002; 95: 588–95.
32 Lai YC, Shih CY, Jeng CM *et al.* Hepatic arterial infusion chemotherapy for hepatocellular carcinoma with portal vein tumor thrombosis. *World J Gastroenterol* 2003; 9: 2666–70.
33 Urabe T, Kaneko S, Matsushita E, Unoura M, Kobayashi K. Clinical pilot study of intrahepatic arterial chemotherapy with methotrexate, 5-fluorouracil, cisplatin, and subcutaneous interferon-alpha-2b for patients with locally advanced hepatocellular carcinoma. *Oncology* 1998; 55: 39–47.
34 Sakon M, Nagano H, Dono K *et al.* Combined intraarterial 5-fluorouracil and subcutaneous interferon-alpha therapy for advanced hepatocellular carcinoma with tumor thrombi in the major portal branches. *Cancer* 2002; 94: 435–42.
35 Ota H, Nagano H, Sakon M *et al.* Treatment of hepatocellular carcinoma with major portal vein thrombosis by combined therapy with subcutaneous interferon-a and intra-arterial 5-fluorouracil: role of type I interferon receptor expression. *Br J Cancer* 2005; 93: 557–64.
36 Obi S, Yoshida H, Toune R *et al.* Combination therapy of intraarterial 5-fluorouracil and systemic interferon-alpha for advanced hepatocellular carcinoma with portal venous invasion. *Cancer* 2006; 106: 1990–7.
37 Kogure T, Ueno Y, Iwasaki T, Shimosegawa T. The efficacy of the combination therapy of 5-fluorouracil, cisplatin and leucovorin for hepatocellular carcinoma and its predictable factors. *Cancer Chemother Pharmacol* 2004; 53: 296–304.
38 Nishiyama M, Yamamoto W, Park JS *et al.* Low-dose cisplatin and 5-fluorouracil in combination can repress increased gene expression of cellular resistance determinants to themselves. *Clin Cancer Res* 1999; 5: 2620–8.